


Spring 5-2014

Study of the Structure-Property Relationships That Determine the Effects of Latexes and Starch Containing Latex Emulsions on the Performance of the Barrier Coatings (Sub-coat) for Paper

JoAnna Marie Monfils
University of Southern Mississippi

Follow this and additional works at: https://aquila.usm.edu/masters_theses

 Part of the [Polymer and Organic Materials Commons](#), [Polymer Chemistry Commons](#), and the [Polymer Science Commons](#)

Recommended Citation

Monfils, JoAnna Marie, "Study of the Structure-Property Relationships That Determine the Effects of Latexes and Starch Containing Latex Emulsions on the Performance of the Barrier Coatings (Sub-coat) for Paper" (2014). *Master's Theses*. 28.

https://aquila.usm.edu/masters_theses/28

This Masters Thesis is brought to you for free and open access by The Aquila Digital Community. It has been accepted for inclusion in Master's Theses by an authorized administrator of The Aquila Digital Community. For more information, please contact Joshua.Cromwell@usm.edu.

The University of Southern Mississippi

STUDY OF THE STRUCTURE-PROPERTY RELATIONSHIPS THAT DETERMINE
THE EFFECTS OF LATEXES AND STARCH CONTAINING LATEX
EMULSIONS ON THE PERFORMANCE OF THE BARRIER
COATINGS (SUB-COAT) FOR PAPER

by

JoAnna Marie Monfils

A Thesis

Submitted to the Graduate School
of The University of Southern Mississippi
in Partial Fulfillment of the Requirements
for the Degree of Master in Science

Approved:

Jeffrey S. Wiggins

Director

Sarah E. Morgan

James W. Rawlins

Maureen A. Ryan

Dean of Graduate School

May 2014

ABSTRACT

STUDY OF THE STRUCTURE-PROPERTY RELATIONSHIPS THAT DETERMINE THE EFFECTS OF LATEXES AND STARCH CONTAINING LATEX EMULSIONS ON THE PERFORMANCE OF THE BARRIER COATINGS (SUB-COAT) FOR PAPER

by JoAnna Marie Monfils

May 2014

The history of carbonless paper dates back to the 1940s. Before this, a carbon copy sheet was needed between sheets of paper to be able to produce one or more copies simultaneously during writing. The pressure from a pen or typewriter would help deposit the ink of the carbon paper onto the blank sheet of paper under the original written sheet to create a “carbon copy.” This method did however, have its disadvantages. Not only did it produce a limited number of copies, but it was also a messy process. So came the creative process of using microencapsulated dyes to make carbonless paper (Burrell, 2003, pp. 451-456). In this process, microencapsulated dyes are coated onto the back of the original sheet so when pressure is applied to the top sheet, it causes the microcapsules to rupture and form an image on the receiver sheet below. Under this capsule coating is a barrier coat or sub-coat, which is applied to the back of the original written sheet. The coating limits the encapsulated dye from absorbing into the original written sheet and increases the dye transferring onto the copy receiver sheet. In the barrier coating, latexes are used. Different chemical properties within the latex will make the barrier coatings perform differently (Mumford, 2007).

The goal of this research study was to test the structure-property relationships that determine the effects of commercial latexes and starch containing latex emulsions (SCEs) on the performance properties of the barrier coating (sub-coat) for paper. The testing of these property changes was performed on the thin film coating of varying pounds per ream on base stock 34lb Domtar paper. Six different latexes with mildly different chemical properties were tested. The rheological techniques used to evaluate the coating slurries include: water retention, viscosity, and pH testing. The performance measurement tests done on the basestock coated samples include: Oil resistance and absorption which were measured through K&N and Croda (Manders Red Drawdown) ink tests and also Sheffield porosity. In conclusion, Typewriter Intensity and Frictional Smudge testing was done to verify the performance results of the barrier coated and CB capsule coated sheets.

Through the performance and verification tests, some general conclusions were determined. These include: an increase in coat weight showed an increase in transfer efficiency and a smaller particle size latex created a better film and more sealed base stock sheet. This was shown not only in the porosity values, but also in the ink absorption results. It was also determined that the acrylonitrile containing latexes performed better due to the creation of a softer more flow-able latex. It was determined that DMF 5501, a commercial latex from Styron containing styrene butadiene copolymer with a low level of carboxylic acid groups, a high level of acrylonitrile groups, T_g 15 °C, and a particle size of 135nm, had the best performance when targeting the lowest coat weight, at 2lbs per ream. The smaller particle size and presence of both carboxylic acid and acrylonitrile groups proved to aid in this performance.

An increase in binder efficiency was shown through testing, it is believed that both of the chemical groups present helped by binding the CB capsule coating to a greater extent to the base stock sheet. The smaller particle size aided in this binding by creating a better flowing more pliable latex which created an evenly formed barrier coat film. The porosity values results determined that DMF 5501 formed a better film, creating a more sealed sheet, hence a showing lower porosity value. The K&N and Croda Ink intensity values also showed that DMF 5501 performed best by showing highest ink intensity values on each base stock sheet. The performance verification tests determined that at only 2 lbs per ream of applied coating, DMF 5501 performed within the required standards set by Appleton Paper Inc., and if chosen, this latex could be used within the current carbonless paper product.

ACKNOWLEDGMENTS

First I would like to thank my graduate research advisor, Dr. Sarah E. Morgan, for her guidance in research direction and continued support, along with her understanding and patience. I would also like to thank my other committee members, James W. Rawlins and Jeffery S. Wiggins. Also my Appleton Papers Inc., research advisor, Dr. Paul Proxmire for giving me an opportunity to do this project and both support and guide me to complete the project successfully. Along him, I would also like to thank Craig Weber for providing guidance and direction in times of need. This work was also supported in collaboration between the University of Southern Mississippi and Appleton Papers Inc.

I would also like to thank my fellow coworkers for their knowledge, patience and continued support throughout my journey. My direct supervisors, both Gary Hart and Robert Bobnock, I would like to thank for their recommendations involved in this research.

Finally, I will close and acknowledge with all the respects and gratitude to my friends and family for their continued support during this time. Last but not least, my husband Adam Monfils and son Kaden deserve special recognition of their wholehearted support of this project, including their daily encouragement to finish and achieve my Master's degree.

TABLE OF CONTENTS

ABSTRACT.....ii

ACKNOWLEDGMENTS.....v

LIST OF TABLES.....vii

LIST OF ILLUSTRATIONS.....viii

LIST OF ABBREVIATIONS.....xi

CHAPTER

I. INTRODUCTION.....1

 Organization

 Literature Review

 Motivation and Contribution to Research

 Research Objectives

II. EXPERIMENTAL.....21

 Materials

 Rheology Testing

 Performance Testing

III. RESULTS AND DISCUSSION.....26

 Rheological Techniques Phase I

 Performance Testing Phase I

 Rheological Techniques Phase II

 Performance Testing Phase II

 Performance Verification Analysis

IV. CONCLUSION.....55

 Future Research Considerations

APPENDIX.....58

REFERENCES59

LIST OF TABLES

Table

1.	Water Retention Summary Phase I.....	26
2.	pH Summary Phase I.....	27
3.	Viscosity Summary Phase I.....	28
4.	Water Retention Summary Phase II.....	35
5.	pH Summary Phase II.....	36
6.	Viscosity Summary Phase II.....	36
7.	Porosity Summary Phase II.....	37
8.	K&N Ink Absorption Summary Phase II.....	38
9.	Croda (Manders Red Drawdown) Ink Absorption Summary Phase II.....	40
10.	2 Minute Typewriter Intensity Imaging Summary.....	49
11.	Frictional Smudge Imaging Summary.....	52

LIST OF ILLUSTRATIONS

Figure

1.	Composition of Carbonless Copy Paper (Appvion, 2013).....	3
2.	Transformation between leuco and colored form of crystal violet lactone (Salamone, n.d., pp. 8369-8374).....	5
3.	Barrier Coating Mechanism (Appleton Papers Inc., 2012).....	8
4.	SEM Images - Coated vs. Uncoated Base Stock Paper	10
5.	Appleton Paper Inc. Carbonless A-Capsule Slurry	14
6.	Styrene Butadiene (Wygant, 2011).....	15
7.	Styrene Acrylic (Zang & Aspler, 1995).....	15
8.	Porosity Summary Phase I.....	29
9.	K&N Ink Absorption Summary Phase I.....	30
10.	Croda (Manders Red Drawdown) Ink Absorption Summary Phase I.....	31
11.	RAP1017NA was drawn down at 3 lbs per ream on (a) Mylar and (b) 34 lb Domtar base stock to see any significant changes in coating topography.....	32
12.	XUR-YM-2013-APBARSCE-1 was drawn down at 3 lbs per ream on (a) Mylar and (b) 34 lb Domtar base stock to see any significant changes in coating topography.....	32
13.	XU 31524.00 was drawn down at 3 lbs per ream on (a) Mylar and (b) 34 lb Domtar base stock to see any significant changes in coating topography.....	33
14.	RAP 810NA was drawn down at 3 lbs per ream on (a) Mylar and (b) 34 lb Domtar base stock to see any significant changes in coating topography.....	33
15.	DMF 5501 was drawn down at 3 lbs per ream on (a) Mylar and (b) 34 lb Domtar base stock to see any significant changes in coating topography.....	33
16.	SCE 5615 was drawn down at 3 lbs per ream on (a) Mylar and (b) 34 lb Domtar base stock to see any significant changes in coating topography.....	34

17.	RAP1017NA was drawn down at 2 lbs per ream on (a) Mylar and (b) 34 lb Domtar base stock to see any significant changes in coating topography.....	41
18.	RAP1017NA was drawn down at 3 lbs per ream on (a) Mylar and (b) 34 lb Domtar base stock to see any significant changes in coating topography.....	41
19.	RAP1017NA was drawn down at 5 lbs per ream on (a) Mylar and (b) 34 lb Domtar base stock to see any significant changes in coating topography.....	42
20.	RAP 810NA was drawn down at 2 lbs per ream on (a) Mylar and (b) 34 lb Domtar base stock to see any significant changes in coating topography.....	42
21.	RAP 810NA was drawn down at 3 lbs per ream on (a) Mylar and (b) 34 lb Domtar base stock to see any significant changes in coating topography.....	42
22.	RAP 810NA was drawn down at 5 lbs per ream on (a) Mylar and (b) 34 lb Domtar base stock to see any significant changes in coating topography.....	43
23.	DMF 5501 was drawn down at 2 lbs per ream on (a) Mylar and (b) 34 lb Domtar base stock to see any significant changes in coating topography.....	43
24.	DMF 5501 was drawn down at 3 lbs per ream on (a) Mylar and (b) 34 lb Domtar base stock to see any significant changes in coating topography.....	43
25.	DMF 5501 was drawn down at 5 lbs per ream on (a) Mylar and (b) 34 lb Domtar base stock to see any significant changes in coating topography.....	44
26.	SCE 5615 was drawn down at 2 lbs per ream on (a) Mylar and (b) 34 lb Domtar base stock to see any significant changes in coating topography.....	44
27.	SCE 5615 was drawn down at 3 lbs per ream on (a) Mylar and (b) 34 lb Domtar base stock to see any significant changes in coating topography.....	44
28.	SCE 5615 was drawn down at 5 lbs per ream on (a) Mylar and (b) 34 lb Domtar base stock to see any significant changes in coating topography.....	45
29.	Box plot of Porosity.....	46
30.	Box plot of K&N Ink.....	47
31.	Box plot of Croda Ink.....	48
32.	Typewriter Intensity Sample Images - Images going from top to bottom, RAP1017NA, RAP 810NA, DMF 5501 and SCE 5615.....	51

33. Frictional Smudge Sample Images - Images going from left to right,
RAP1017NA, RAP 810NA, DMF 5501 and SCE 5615.....53

LIST OF ABBREVIATIONS

API	Appleton Papers Inc.
SCE	Starch Containing Emulsion
CB	Coated Back
CF	Coated Front
NCR	No Carbon Required
cP	Centipoises
SU	Sheffield Units
psi	Pounds per Square Inch
RPM	Rotations per Minute
lb	Pound
mL	Milliliters
F	Fahrenheit
C	Celsius
mm	Millimeters

CHAPTER I

INTRODUCTION

Organization

This thesis is organized into four chapters. Chapter I is a general introduction to carbonless paper, its uses and how it works. Barrier coatings and starch containing emulsions are described, along with how and why they work so well for carbonless paper products. Chapter II describes the experiments performed and how the mechanical and rheological properties of the samples were analyzed. Chapter III discusses the results of the samples analyzed in detail. Finally, Chapter IV presents the conclusions of the research results and future research opportunities.

Literature Review

Carbonless Paper

Before carbonless paper was invented, a carbon copy sheet was needed between sheets of paper to produce one or more copies simultaneously during writing. This paper was called carbon paper, and it is coated on one side with a layer of loosely bound dry ink. In use, this carbon paper is placed between the original and a second sheet of paper onto which it is to be copied. The carbon paper creates a copy when the user writes or types on the original sheet. The pressure from the typewriter or pen helps to deposit the ink of the carbon paper on-to the blank sheet, thus creating a “carbon copy” of the original document. This process did work well, however, it did have its disadvantages; it could only produce a limited number of copies and was often messy when putting a sheet of carbon paper between the sheets of paper (Laurence, 1995). Also if the carbon sheet happened to be misplaced or lost, no copies could be made at all. There was also extra

waste associated with the disposal of the carbon paper. Although valuable information could be obtained from the carbon paper, these disadvantages are what ultimately led to the creation of carbonless paper.

The history of carbonless paper dates back to the late 1940s. Researchers, by the name of Lowell Schleicher and Barry Green (working for NCR Corporation, later known as Appleton Papers Inc.) found a need for printing without the use of carbon paper and began to develop a technique for doing such. NCR paper, or “no carbon required,” is another term for carbonless paper. Carbonless paper simply creates a copy of the handwritten (or mechanically typed) portion of a document without the use of carbon paper, printer, photocopier, or any other electrical devices (Appvion, 2013; Mumford, 2007). The key to achieving this goal was the development of how to convert dyes to their colorless state. Dyes in their colorless state will produce no image on plain paper, clothing, or skin, but when the colorless dyes come into contact with a reactive chemical coating, the image is then formed. Once the dyes were converted to their colorless precursor, it was necessary to develop a medium with the reactive coating that could be applied on paper. The paper medium would need to produce an intense and complete color transfer, only producing an image where pressure was applied; this led to the use of microencapsulated dyes (Appleton Papers Inc., 1989). The image produced on the copy of the carbonless paper form must have good transferability to form an intense, meaning dark, and complete, meaning fully reacted color transfer. Without this quality of ink transfer, there will not be a clear-cut image for readers to see (Appvion, 2013).

Carbonless paper has different parts. The top sheet of paper is called the “CB” or coated back. This is the top sheet and the original handwritten (or mechanically typed)

copy (Appvion, 2013). On the reverse side of this sheet there is a back coating consisting of millions of microcapsules of dissolved colorless color formers (dyes) (Glatthaar, 2011). These dyes are indefinitely sealed with the polymer shell of the microcapsule, only to be broken upon applied pressure. The barrier coating is also applied to the underside of this sheet before the layer of microencapsulated dye is applied. The sheet under the CB is the “CF” or coated front. This part of the sheet is also called the receiver sheet and is used as the copy of the handwritten CB sheet. This sheet is coated with a reactive resin coating. This coating reacts with the colorless dyes to form a permanent image on the topside of this receiver sheet, CF surface (Appleton Papers Inc., 1989).

Figure 1 below shows a diagram of the carbonless copy paper, both the positioning of the described sheets and the existing coatings that are applied to each sheet.

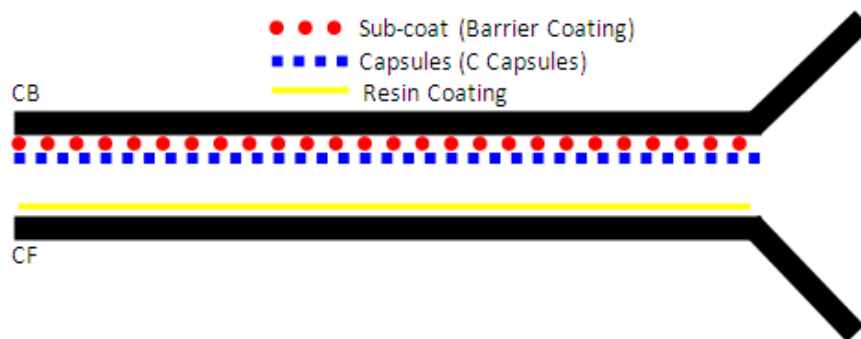


Figure 1. Composition of Carbonless Copy Paper (Appvion, 2013).

Carbonless paper works by the simple application of pressure. When pressure from a pen or any writing device creates pressure on the top sheet of the carbonless paper, the pressure applied causes the microencapsulated colorless dye on the back side of the sheet of paper to break and transfer the colorless dye onto the front of the receiver sheet (Mumford, 2007). When the colorless dye comes into contact with the reactive acidic coating on the front of the back sheet, the dye reacts to form an intense darkened

image, therefore creating a permanent mark on the front of the receiver sheet, hence creating a copy of the handwritten top sheet (Appvion, 2013; Karukstis & Vanlecke, 2003). An accurate image is created because of small sized capsules, usually between 3 to 8 microns, containing the dye (White, 1998, pp. 1119-1120). Carbonless paper can also be manufactured to create multiple copies, up to 5, of the original CB, handwritten sheet (Mumford, 2007).

The chemical reaction taking place between the two sheets of carbonless paper requires that the coatings on both the CB and CF sheets function properly. The coating on the CB sheet contains the barrier coating, and a color former, or leuco dye (literally meaning “white dye”), which becomes colored when the dye breaks from the polymer shell and reacts with hydrogen from the acidic coating on the CF reactive resin coated sheet. This change involves hybridization from an sp^3 to an sp^2 orbital in the dye, and delocalization within the planar aromatic structure of the cationic product lowers the electronic excited states from being in the original UV range to now being in the visible range for the protonated product (White, 1998, pp. 1119-1120).

A more in-depth explanation of the chemical reaction that is taking place between the CB and CF sheet to form an image can be explained using a dye called crystal violet lactone. The microencapsulated slightly yellow, leuco/colorless dye crystal violet lactone is found on the CB capsule coated side of the sheet on top of an already placed barrier coating. When pressure is applied to the carbonless paper form, the microcapsules containing the leuco dye are broken. The barrier coating on the CB sheet limits the dye from depositing on the CB sheet; instead the dye is transferred to the CF sheet coated with phenolic resin or reactive clay. When the crystal violet lactone comes into contact

with the acidic reactive coating, the acid donates a proton, hence converting the colorless dye to a red-black image. The structural change occurring in this reaction is shown in Figure 2 below. In this case, the fluoran structure of the crystal violet lactone becomes colored as a result of the acid-induced cleavage of the phthalide bond (Salamone, n.d., pp. 8369-8374).

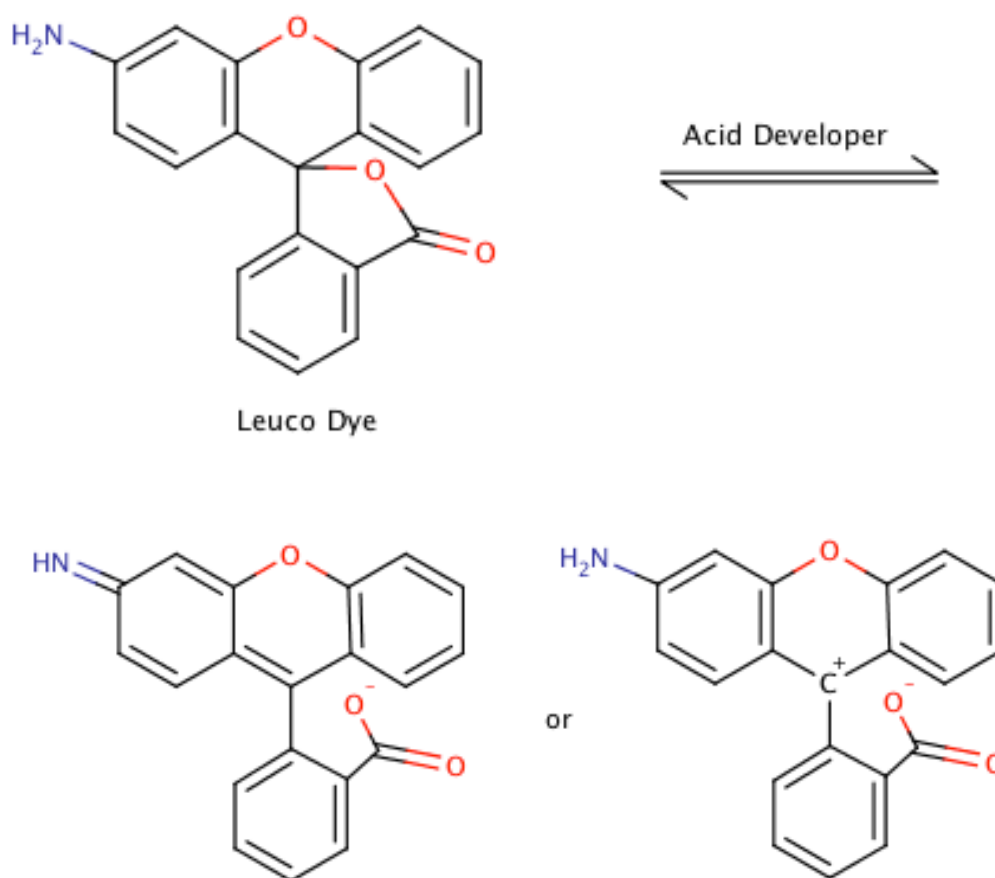


Figure 2. Transformation between leuco and colored form of crystal violet lactone (Salamone, n.d., pp. 8369-8374).

Barrier Coatings (sub-coat)

Barrier coatings are commonly used in food packaging, electrical devices, and many other currently used items today. Typically a barrier coating is impervious to oxygen and water, keeping food from spoiling or water from penetrating to the electronic device.

For a carbonless barrier coating, an aqueous dispersion of fine polymer particles is applied to the uncoated surface of carbonless paper before any coating of microcapsules is added. A barrier coating is formed onto a base stock sheet of paper through the use of a film-forming latex (Scott & Trosset, 1989). The barrier coating's main function is to prevent the solution of leuco dyes from absorbing into the CB sheet, and it promotes transfer to the CF layer of the sheet below. A barrier coating can be constructed by using pure latexes; however this can become highly expensive. This is why clays and starches are added to the mixture. When a clay is introduced into the coating, the platelet-like shape of the clay improves the barrier property by increasing tortuosity. Tortuosity is often used to describe a barrier to diffusion in porous media, meaning having many turns and twists. Not only does tortuosity have the potential to introduce a significant cost savings, but it may also improve the barrier properties.

A series of tests are done on each of the coatings before they are drawn down on a sheet of paper. These include measurements of percent solids, pH, viscosity and water retention. Percent solids are the percent ratio of the mass amount of suspended and dissolved solids within a total solution. pH is the measure of acidity or basicity of an aqueous solution. Viscosity is the measurement of the resistance of a fluid to shear stress.

Water retention is defined as the fibers ability to absorb water and swell. This test is used to measure coating de-watering under pressure.

The barrier coating mixture involves many different components; however, only those that have significant effect on the properties of the coating will be described. These are clays, starch, latex, resin, and viscosity modifiers. The clay or other mineral pigments in the coating help to improve the print quality, gloss, brightness and opacity of the finished product (Bollstrom, Tuominen, Maattanen, Peltonen, & Toivakka, 2011). These qualities are only some of the important properties that must be achieved to have a good quality finished product for consumers. Gloss, brightness and opacity are properties related to the general appearance of the product, whereas print quality is how well the product performs when ink is introduced into the system. Starch acts as a binder. This binder not only helps adhere the barrier coating to the paper, but also the capsule containing coating to the barrier coating. Starch has also been known to help increase the strength of the final paper product by contributing to the stiffness and bonding within the sheet due to the bonding of the starch particles themselves. Dispersed polymers or latexes are used in barrier coatings to improve barrier properties, which control diffusion of water vapor and oxygen and the rate of ink absorption (Burrell, 2003, pp. 451-456). The latex is considered the most important material for creating a sealed layer against ink absorption. The resin is used as an anionic dispersant. A viscosity modifier is also added to the coating to improve the performance of the coating over a wide temperature range (i.e. use on coaters with higher temperatures and when used at room temperature when making hand coatings). These slurry coatings are then applied to sheets of paper to produce carbonless paper products. Typical coat weight values for the barrier coating are

between 2-15 g/m² depending on the components within the coating and product application.

The barrier coating mechanism is described using this equation (Appleton Papers Inc., 2012):

$$\text{Permeability} = \text{Solubility} \times \text{Diffusion}$$

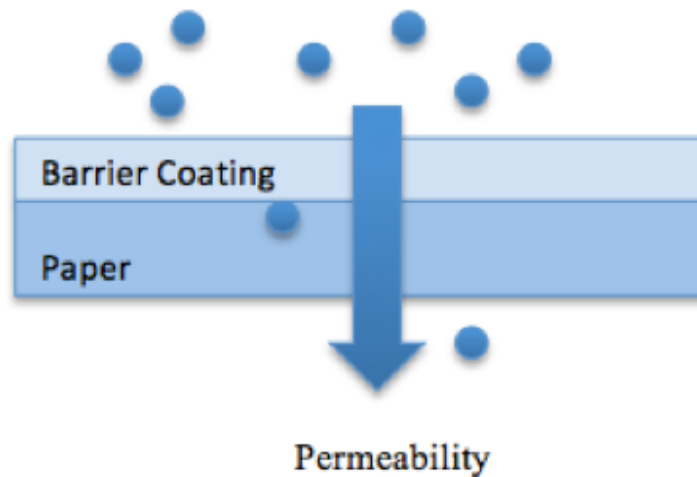


Figure 3. Barrier Coating Mechanism (Appleton Papers Inc., 2012).

Diffusion is defined as penetration of the molecules into the film, as they try to reach equilibrium. Solubility is defined as the how well a substance can dissolve within a solvent. A good barrier performance is dependent on the type of penetrant and on the properties of the coating. Figure 3 is used to describe this barrier coating mechanism that is taking place when the ink is released from the microcapsules. Due to the barrier coating on the sheet, very little ink would transfer back into the CB sheet, creating a better transfer to the copy, receiver CF sheet.

A good barrier coating requires a polymeric system with the following general properties (Kjellgren, 2008):

- A high glass transition temperature (T_g) – give low mobility of the chain segments, hence, creating fewer voids in the matrix and a more tortuous structure
- High chain stiffness and high chain packing – increases the crystallinity of the polymer, hence, lower permeability
- The bonding attraction between the chains must be able to resist mobility – lowers permeability
- Inertness to the permeant – if moisture is absorbed, it can create a plasticizing effect, this in turn can lower T_g , hence increasing the permeability of the coated sheet

The important properties for the best barrier coating performance are analyzed through tests such as: porosity (Sheffield, TAPPI Method T-547, API Method 10010.01) and ink absorption testing. This testing is measured using standard tests known as Croda Ink (Manders Red Drawdown API Test Method 10013.22) and K&N Ink (API Method 10013.07). Standardized Manders Red Ink is supplied from Flint Ink (Ann Arbor, MI) and calibrated by the Analytical Services Department at Appleton Inc. Lot number of the Flint Ink Red Drawdown Ink MBR10039-050 was #55857 with a specified 2-minute absorption time. Standardized K&N Ink is supplied from K&N Laboratory Inc. (La Grange, IL) and calibrated by the Analytical Services Department at Appleton Inc. Lot number of the K&N ink was #X.99 with a specified 10 second absorption time. Ordinary paper is generally 50% air, by volume (Wygant, 2011). Most of the air within the sheet resides within its porous structure, however a little of the air is present within the fibers. The porosity of the sheet is defined as the ratio of pore volume to the total volume of the

sheet. The measurement is determined by how easily air passes through the sheet (Scott & Trosset, 1989). Porosity is an important property for determining whether a good or bad barrier coating exists. Poor porosity will allow ink and other coating materials to penetrate into the CB sheet. Determining the correct porosity value for the desired product outcome is just one step in producing a high performing barrier coating. Figure 4 below shows SEM images of what an uncoated base stock sheet looks like versus a coated base stock sheet. These images show how much more porous the uncoated sheet is when compared to the coated sheet.

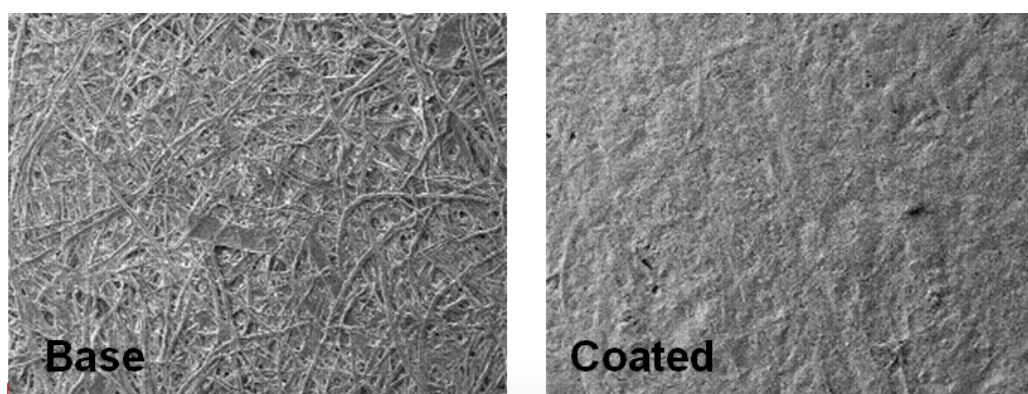


Figure 4. SEM Images – uncoated (base) vs. coated base stock paper.

The other tests, Croda (Manders Red Drawdown API Test Method 10013.22) and K&N ink (API Test Method 10013.07) are staining techniques to help characterize ink absorption. Ink absorption is defined as the ability to absorb or accept ink. These techniques also emphasize the structure and porosity of the coatings. Coatings that are more porous show a darker color when tested, hence having the ability to absorb larger quantities of the ink (Wygant, 2011). The Croda ink (Manders Red Drawdown API Test Method 10013.22) test involves a thick film of red tacky dye, which is applied on the surface of the coated paper and allowed to penetrate for 2 minutes. After the two minutes, excess ink is wiped from the surface using a soft cotton pad. The reflectance of the stain

is then measured using an opacimeter (Zang & Aspler, 1995). The K&N ink (API Test Method 10013.07) test helps to determine surface printability. This test involves tracing a square on the coated sheet of paper. The gray colored ink is then applied using a small spatula to the full area of the square and allowed to penetrate the sheet for 10 seconds. After the ten seconds, the ink is quickly removed using the small spatula and then wiped with a soft cotton pad. The ink absorbency is then measured using an opacimeter to determine depth of absorbency of the ink within the sheet ("Tappi Routine Control Methods," n.d.). In general, these ink smears are used to help evaluate the receptivity of the paper surface to oil based ink. The tests are intended to specify a general level of absorbency and any deviation in absorbency or mottle tendency. For testing the barrier coating, a low level of absorbency would be consistent with a good barrier coating property. These ink tests are important in determining the absorbance property associated with barrier coatings. The main goal of barrier coatings is to repel ink and keep it from going into the fibers of the sheet.

The concluding imaging verification tests are performed on barrier (sub-coat) and microencapsulated dye coated samples, including the 2 Minute Typewriter Intensity test (API Test Method 20001.12) and the Frictional Smudge test (API Test Method 20002.01). The 2 Minute Typewriter Intensity test (API Test Method 20001.12) measures the image capability of the coated paper (CF, CB or SC). The method uses a 6 x 5 in. sheet of CB and CF paper which is sandwiched together and printed with test pattern that is competed by a typewriter. This test compares the imaged area to the unimaged area of the sheet to determine the darkness of the image after 2 minutes of development time. This test is important in determining if the intensity caused by the reaction is too cold. If

so, the intensity is too weak, causing the image to be light and the development does not occur fast enough. If it is too hot, the image develops too easily resulting in unintentional imaging or smudge. The Frictional Smudge test (API Test Method 20002.01) gauges the robustness of the coating by measuring the intensity of an image created by frictional forces. This method tests the CF and CB surfaces when rubbed against each other. A strip of each CB and CF paper is needed in 2 1/8" wide x 13" long dimensions. The CF sample is positioned on the load arm and the CB sample of the drum. When the drum rotates, the CF and CB sheet make contact with no applied pressure. After contact, the image paper is removed from the load arm (CF) and allowed to develop for two minutes before reading. The imaged area versus the unimage area is then read using an opacimeter. A discoloration on the CF coated side can occur on the carbonless paper when it is brought in tight, sliding contact with the CB coating. This type of contact can happen when winding up rolls of coated paper. The image intensity cannot be so sensitive that it results in accidental or premature breakage from handling or further conversion in the packaging, printing or sheeting process.

Microencapsulation

Microencapsulation was the key development that led to the invention of carbonless paper. Microencapsulation is described as the shielding of an active ingredient (core material) within a protective shell. Utilizing the principles of colloid chemistry, the colorless, or leuco dye solution preformed at its highest when encapsulated within a polymer shell called "capsules." These capsules or shells are created through several different chemical reactions. Which shell material to choose is dependent not only on the chemistry of the core, but also the desired use of the capsules.

The most basic process of development begins by creating a homogenous mixture of colorless (leuco) dyes dissolved in oils and mixed with aqueous solutions to form an emulsion of properly sized dye-oil droplets. The next process involves depositing a thin polymer shell, or protective wall at the interface to surround each of the dye-oil droplets. To finish the chemical process, a curing or hardening reaction takes place to fully form the dye-oil containing microcapsules (Appleton Papers Inc., 1989). The mixture of dye-oil containing microcapsules, along with the barrier coating (sub-coat) are then coated to the underside of the CB sheet. Figure 5 below shows an SEM image taken of the dye containing microcapsules that are applied to the coating on a CB sheet. These capsules, which are within the carbonless paper coating, rely on mechanical rupture of the capsules by applying pressure to the sheet (Karukstis & Vanlecke, 2003).

The other process often talked about in microencapsulation is the coacervation process. Coacervation is defined, by IUPAC, as the separation of colloidal systems into two liquid phases. It is to be distinguished from precipitation, which is observed in the form of coagulum or flocs and occurs in colloidally unstable systems (Everett, 1992, pp. 44). This process occurs when the active core material is added to a homogenous solvent and polymer solution. The solution is then agitated to disperse the immiscible core material. In doing this tiny droplets are created within the homogenous emulsion. Reactions taking place within this emulsion are then initiated by changing the temperature and/or pH (or on addition of other reactive materials) of this emulsion. The goal is to create two incompatible liquid phases, each containing different amounts of the solubilized polymer. There are two phases that will result from this, a supernatant, containing a low concentration of polymers, and a coacervate phase, containing a higher

concentration of polymers. The coacervate phase is appropriately selected to absorb onto the surface of the dispersed core material droplets to form the shell. The fluid film is then deposited; however the hardening of the shell still must occur. This is usually done using a cross linking agent through further chemical reaction and/or a temperature increase or decrease. After the reaction has taken place, the microcapsules will settle and separate, however structuring agents can be used to help stabilize the mixture (Karukstis & Vanlecke, 2003).

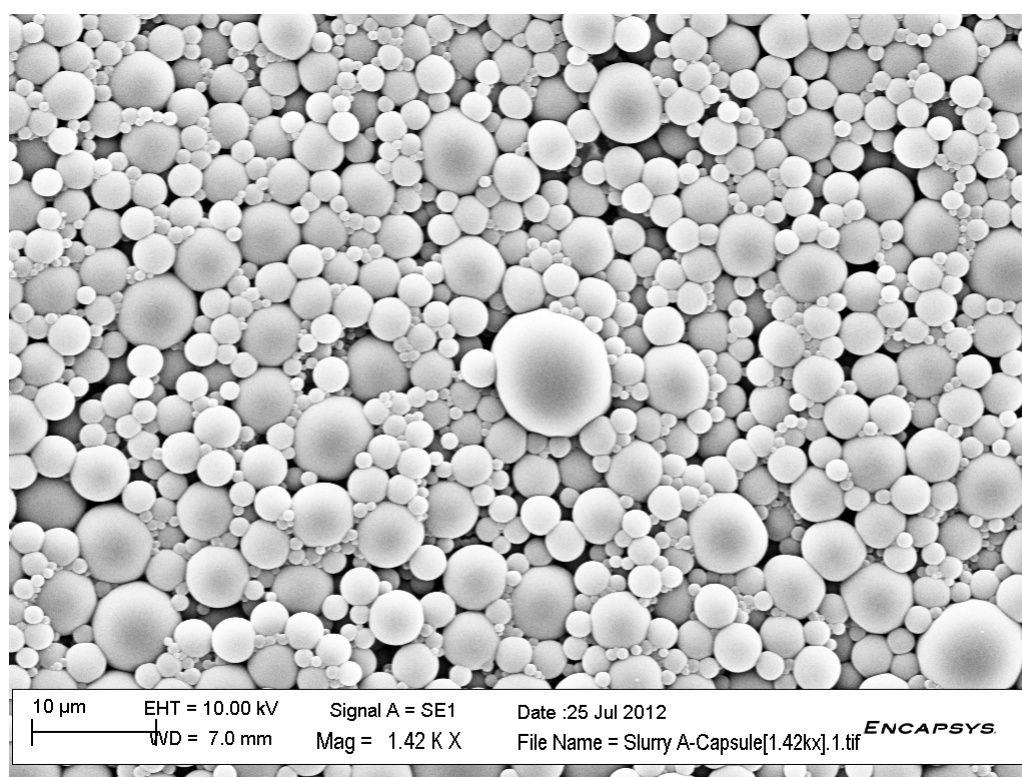


Figure 5. SEM Image – Appleton Paper Inc. Carbonless A-Capsule Slurry.

Once the slurry microcapsule coating of leuco dyes are created, these capsules slurries are commonly drawn down on a basestock sheet. The concentration of coating applied is often in a range of 2-5 lbs per ream on top of a barrier coated sheet.

Latexes & Starch Containing Emulsion Latexes (SCEs)

Latex is the film-forming, stable emulsion of polymer micro-particles used in the barrier coatings. There are two different chemical structures of latexes used in this study, styrene butadiene copolymers (SB), seen in Figure 6, and styrene acrylic copolymers (SA), seen in Figure 7.

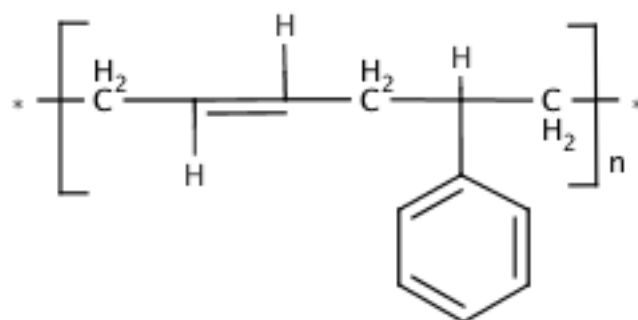


Figure 6. Styrene Butadiene (Wygant, 2011).

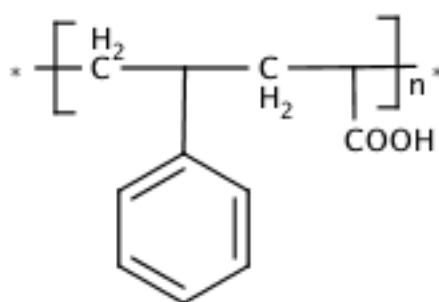


Figure 7. Styrene Acrylic (Zang & Aspler, 1995).

Styrene butadiene (SB) copolymers have been known to increase strength of the coating, the printability, and the fiber bonding and bond strength. A range of relative concentrations of styrene to butadiene can be made, although the typical mixture is

approximately 75% butadiene and 25% styrene. Styrene acrylic (SA) copolymers are often used in comparison to SB copolymers because they are known to improve flexibility and adhesion. SA copolymers are also known for their durability to environmental exposure such as their resistance to ultraviolet degradation. Different concentrations of each co monomer are used to vary the properties needed in the latex. The higher content of styrene within the copolymer will increase the T_g of the latex. Particle size and molecular weight of the latexes are mainly controlled through the process of emulsion polymerization. Emulsion polymerization is used to give the latex stability; this is achieved through the use of an emulsifier composed mainly of a hydrophilic and a hydrophobic portion (Blackley, 1975; Tracton, 2007). Often acrylonitrile and carboxylic acid groups are added to these latexes to improve the stability and increase adhesion along with other properties that may be needed.

Carboxylated latexes contain a small amount of unsaturated carboxylic acids. These latexes tend to have high gel content, better thermal stability, improved abrasion resistance and easier process ability. When carboxylic acid groups are present within the latex that is included in the barrier coating, the acid groups that are on or near the fiber sheet surface have an increased bond strength with the fibers. This bond strength increases the binding ability of the coating to the base stock sheet. Latexes can also contain acrylonitrile groups. The acrylonitrile groups are often incorporated from vinyl nitrile copolymers (Dillard & Pocius, 2002). Acrylonitrile groups are very polar molecules due to their lack of symmetry. When present within the latex, hydrogen bonding develops very strongly. This increased bond strength interacts with the sheet

fibers and other coating ingredients to produce hydrogen bonds and improve the binding ability of the latex to the base stock sheet (Hertz & Bussem, 1994).

Starch plays a major role in both the CB barrier coating and microcapsule coating. Starch not only acts as a binder to help the barrier coating bind to the capsule coating, but it can also increase the strength of the end product (Burrell, 2003, pp. 451-456). Use of a starch containing emulsion with the correct starch content has the potential to simplify and reduce the cost in the coating process. Instead of adding starch to each coating formulation separately, SCEs can be used to eliminate the starch addition step. Starch containing latexes might offer significant cost savings, along with improved barrier properties (Bollstrom, Nyqvist, Preston, Salminen, & Toivakka, 2013).

In this study, it was proposed to evaluate six different latexes that contain mildly different levels of starch, acrylonitrile groups, carboxylic acid groups, and different glass transition temperatures. These commercial latexes are as follows:

1. RAP 1017NA Latex: styrene butadiene with a moderate level of carboxylic acid groups, T_g -6°C , and a particle size of 230nm.
2. XUR-YM-2013-APBARSCE-1 Experimental Latex: styrene butadiene starch containing emulsion with a moderate level of carboxylic acid groups, T_g -4°C , and a particle size of 230nm.
3. XU 31524.00 Experimental Latex: styrene butadiene with a low level of carboxylic acid groups, T_g 17°C , and a particle size of 125nm.
4. RAP 810NA Latex: styrene acrylic with a moderate level of carboxylic acid groups, a high level of acrylonitrile groups, T_g -2°C , and a particle size of 155nm.

5. DMF 5501 Latex: styrene butadiene with a low level of carboxylic acid groups, a high level of acrylonitrile groups, T_g 15°C, and a particle size of 135nm.
6. SCE 5615 Experimental Latex: styrene butadiene starch containing emulsion with a moderate level of carboxylic acid groups, a high level of acrylonitrile groups, T_g 14°C, and a particle size of 135nm.

These latexes were chosen to directly compare the effects of changing individual parameters on the performance of the barrier coating.

These six latexes are used in similar concentration within each barrier coating created to be drawn down on base stock sheets. It is hypothesized that some properties of both the latexes and SCE latexes will help produce better barrier properties. These properties include:

- Nitriles help with better binding, hence a softer, more pliable latex with higher strength
- Carboxylic acid groups also help with the binding
- Smaller particle size is usually preferred, however this could also create a more mobile particles

This research study will determine with experimental data how the formulation changes and resulting film properties affect the performance of the current barrier coating (sub-coat) used at Appleton Papers Inc. Performance will be correlated with the structural variations in the polymer latexes.

Motivation and Contribution to Research

The currently used barrier coating (sub-coat) exhibits dye transfer inefficiency. The dye transfer rate has been shown to be 20-25%, while a transfer rate of 40-50% is desired. It has been proven that the openness [porosity] of the barrier coating has a direct correlation with the efficiency of dye transfer. It is hypothesized that reducing the porosity of the barrier coating through control of the coating formulation will improve dye transfer efficiency rates. Specifically, it is believed that a lower T_g polymer binder will provide better film formation, reduce the chain mobility, and increase chain packing, thereby producing better barrier properties. With lower T_g latexes, it is also hypothesized that latexes containing nitrile groups will have better binding efficiency by creating softer, higher strength film. Latexes also containing carboxylic acid groups are known to help the binding properties of the film formation to the base stock sheet. Particle size can also affect the film formation for these barrier coatings. A small particle size usually is superior, but it can have a negative affect by making the particle more mobile. The main goal to be achieved through this research is to define the structure-property relationships that could deliver an improved barrier coating that not only is an efficient film former and dye transferor, but also provides a cost reduction.

Research Objectives

The objectives of this research are as follows:

- Investigate effects of different latex/starch containing emulsions (SCEs) on improving barrier coating (sub-coat) efficiency;
- Use 6 different latexes, one being the control, two of them being SCEs;

- Determine how SCEs/latexes modify rheological properties through Water Retention, Viscosity, and pH testing;
- Compare property effects on the CB sheet through Sheffield Porosity testing, TAPPI Method T-547 (API Method 10010.01) to the control latex currently in use;
- Compare property effects on the CB sheet through K&N Ink Test (API Method 10013.07) to the control latex currently in use;
- Compare property effects on the CB sheet through Manders Red Drawdown Ink [Croda Ink] (API Method 10013.22) to the control latex currently in use;
and
- Define structure-property relationships that determine why these effects occur on the CB sheet properties, using the SCEs/latexes;
- Application of a capsule coating to the pre-coated barrier coating samples to verify results through Typewriter Intensity and Frictional Smudge testing.

CHAPTER II

EXPERIMENTAL

Materials

Six different latexes with mildly different chemical properties were obtained from Styron and used in this study. There are two different chemical structures of latexes used, styrene butadiene copolymers (SB), seen in Figure 6, and styrene acrylic copolymers (SA), seen in Figure 7. RAP 1017NA Latex, donated by Styron, is a styrene butadiene latex with a moderate level of carboxylic acid groups, a particle size of 230nm, 48.8% solids, pH 8, T_g -6°C, MMFT 9°C, and 87% Gel. XUR-YM-2013-APBARSCE-1 Experimental Latex, donated by Styron, is a styrene butadiene starch containing emulsion with a moderate level of carboxylic acid groups, a particle size of 230nm, 48.3% solids, pH 7.5, T_g -4°C, MMFT 10°C, and 86% Gel. XU 31524.00 Experimental Latex, donated by Styron, is a styrene butadiene with a low level of carboxylic acid groups, a particle size of 125nm, 52% solids, pH 8, T_g 17°C, MMFT 17°C, and 86% Gel. RAP 810NA Latex, donated by Styron, is a styrene acrylic latex with a moderate level of carboxylic acid groups, a high level of acrylonitrile groups, a particle size of 155nm, 48% solids, pH 6.5, T_g -2°C, MMFT 2°C, and 91% Gel. DMF 5501 Latex, donated by Styron, is a styrene butadiene latex with a low level of carboxylic acid groups, a high level of acrylonitrile groups, a particle size of 135nm, 49% solids, pH 6.5, T_g 15°C, MMFT 18°C, and 83% Gel. SCE 5615 Experimental Latex, donated by Styron, is a styrene butadiene starch containing emulsion with a moderate level of carboxylic acid groups, a high level of acrylonitrile groups, a particle size of 135nm, 50% solids, pH 6.5, T_g 14°C, MMFT 18°C, and 80% Gel. Hercules CMC 7MT diluted to a 2.2% solids solution (sodium

caroxymethylcellulose) was purchased from Ashland Inc (USA). Colloid 211 (sodium polyacrylate blend) was purchased from Kemira Chemicals, Inc (USA). Ultra Cote Slurry (hydrous aluminum silicate) was purchased from BASF (USA). Modified Ethylated corn starch was purchased from Cargill in dry form and cooked to a 28% solids solution. Z-30 capsules were obtained from Appleton Papers Inc. (Appleton, WI). All chemicals were used as received. (see Appendix)

Coating Makeup

The barrier coatings were made using proprietary ratios. Each ratio will be called X%, Y% and Z% for the coating make-ups. To each coating, X% was made up using Ultra Cote Slurry, CMC 7MT solution, Colloid 211 and water. Y% consists of ethylated cornstarch and Z% of latex. Each coating was made to produce 130 grams of coating and diluted to 21% solids. They were then kept in the refrigerator at 7.5°C to avoid degradation.

Rheology Testing

pH

pH was measured using a Denver Instrument pH Meter. This instrument is calibrated each day, using reference standards pH 7 and pH 4 purchased from Fisher Scientific.

Brookfield Viscosity

Viscosity was measured using a Brookfield DV-E Viscometer. Each sample was run three times using number 63 spindle at 60 rpms for roughly 1 minute. Measurements were recorded in units of centipoises (cP).

Gravimetric Water Retention

The water retention values were measured using an AA-GWR Gravimetric Water Retention Meter. The compressed nitrogen used was obtained from Airgas. The regulated pressure was between 10-15 psi and was held constant for all samples tested. Each sample was tested three times at roughly 2 minutes per sample. The measured unit was reported as gm/m².

Drawdown Process

Phase I Drawdowns were performed using a 34 lb 11 x 16 in. base stock sheet of paper supplied from Domtar; Domtar base stock lot #8055 felt side up. Each coating was sufficiently mixed until homogenous in nature. One pipette, roughly 2 mLs full of coating, was applied to the top of the 34 lb 11 x 16 in. base stock sheet of paper and pushed down the paper using a number three rod to target three pounds per ream. The coating was then dried using a Master Heat Gun obtained from Masters Appliance Corporation; Model: HG-301A with a heat range of 300-500 °F. Once dried, the 11 x 16 in. sheet was cut down to a 10 x 14 in. sheet. This 10 x 14 in. sheet was then used for further testing.

Phase II Drawdowns were performed using the same materials as the Phase I drawdowns, however, the target weights were two, three, and five pounds per ream on both Mylar and 34 lb Domtar base stock.

Performance Testing

Sheffield Porosity

Sheffield Porosity was tested on each coated paper sample. This testing method follows TAPPI Test Method U524. The Lorentzen and Wettre L&W Air Permeance

Tester was used with an air supply ranging from 60 to 125 psi. Each sample was read three times and reported in Sheffield units (SU).

K&N Ink Test

The K&N Ink Test was performed on each coated paper sample using the API Test Method 10013.07. Standardized K&N Ink is supplied from K&N Laboratory Inc. (La Grange, IL) and calibrated by the Analytical Services Department at Appvion Inc. Lot number of the K&N ink was #X.99 with a specified 10 second absorption time was used in this study. The degree of reflectance is obtained using Technidyne BNL-3 Opacimeter within 5 minutes after removing the ink. The degree of absorption is obtained by subtracting the degree of reflectance meter reading from 100.

Manders Red Drawdown (Croda) Ink

Manders Red Drawdown Ink was performed on each coated paper sample using API Test Method 10013.22. Standardized Manders Red Ink is supplied from Flint Ink (Ann Arbor, MI) and calibrated by the Analytical Services Department at Appvion Inc. Lot number of the Flint Ink Red Drawdown Ink MBR10039-050 was #55857 with a specified 2 minute absorption time was used in this study. The average contrast reading is then read using a Technidyne BNL-3 Opacimeter and recorded within 5 minutes after removing the ink.

Surface Analysis (Scanning Electron Microscopy)

Surface morphological images of each sample were taken using a Carl Zeiss Scanning Electron Microscope EVO MA10. Each samples was adhered to a metal stud and sputter coated, using a Denton Vacuum Desk II sputter coater, with a 5 nm thick gold platinum coating under an argon atmosphere. The SEM analysis was performed using

gun settings as follows: 10 kV accelerated voltage, 2.773 A fill target, 50.0 uA beam emission current, 50 pA probe current, a spot size of 351 and a 30 micron aperture size. Pictures of Mylar samples were taken at a 2.5 kx magnification and a working distance of 6.5 mm. Pictures of the coated papers were taken at a 650 x magnification and a working distance of 6.5 mm.

Typewriter Intensity

After samples were coated with the barrier (sub-coat) and capsule coatings, performance verification was done with the 2 minute Typewriter Intensity (API Test Method 20001.12) image test. A Swintec 7003, model number OZ300340 was used, along with CF 15# Superior, CF standard 9/04 reference material. Each sample was tested and allowed to sit for a 2 minute development time. The average intensity was then read using a Technidyne BNL-3 Opacimeter and recorded.

Frictional Smudge

Frictional smudge image testing was done on each sample using a frictional smudge tester developed by API. The API Test Method 20002.01 was used along with CF 15# Superior, CF standard 9/04 reference material. The average smudge value was read using a Technidyne BNL-3 Opacimeter and recorded.

CHAPTER III
RESULTS AND DISCUSSION
Rheological Techniques Phase I

Water Retention

Water retention is used to measure the coating de-watering under pressure and helps to identify the differences in absorptive properties of each different coated paper sample. The water retention value for each coating slurry was determined using an AA-GWR Water Retention instrument and was measured when at 44% solids. Table 1 below shows the water retention summary values for the tested slurries.

Table 1

Water Retention Summary Phase I

Coating Slurry	Water Retention (gm/m ²)
1. RAP1017NA	105.42
2. XUR-YM-2013-APBARSCE-1	100.42
3. XU 31524.00	102.50
4. RAP 810NA	90.00
5. DMF 5501	104.58
6. SCE 5615	155.83

The results above do show minor liquid transferred. There is one significantly higher value observed for the SCE 5615 coating. This may be due to the starch containment within the latex emulsion and this reported value may influence the

performance of this latex. Major increases in the water retention value could greatly affect both the quality and process ability of the coating slurry when the interaction between the base paper and the water phase of the coating occur.

pH

pH was tested on each coating slurry using a pH meter. These slurries were tested at 44% solids. Table 2 below shows a summary of the pH values for the slurries. In general, the last three coatings show lower pH values than the first three coatings in the table below. It appears that the acrylonitrile groups present in the last three latex coatings, play a significant role in the pH value of the coating. This may be due to the lower pH value of 5.0 that exists for acrylonitrile groups.

Table 2

pH Summary Phase I

Coating Slurry	pH
1. RAP1017NA	7.74
2. XUR-YM-2013-APBARSCE-1	7.73
3. XU 31524.00	7.84
4. RAP 810NA	6.88
5. DMF 5501	6.81
6. SCE 5615	6.96

Viscosity

Viscosity plays a big role in paper coatings when adhering the coating to the basestock paper. The viscosity was measured for the coating slurries while at 44% solids.

All values are summarized in Table 3 below. The SCE 5615 showed a significantly lower viscosity value, this could be due to the starch containment within the latex emulsion.

Table 3

Viscosity Summary Phase I

Coating Slurry	Viscosity (cP)
1. RAP1017NA	450
2. XUR-YM-2013-APBARSCE-1	402
3. XU 31524.00	436
4. RAP 810NA	440
5. DMF 5501	390
6. SCE 5615	244

Performance Testing Phase I

Each of these slurry coatings were then drawn down on Domtar 34lb base stock keeping the pounds per ream constant at 3 pounds. The required performance properties were then measured.

Sheffield Porosity

Porosity of the coated sheet was measured using an air permeance meter. This property greatly affects the performance of the barrier coat. In Figure 8 below is a summary of the porosity values for the coated sheets. Both SCE latexes, XUR-YM-2013-APBARSCE-1 and SCE 5615, values were expected to have higher porosity values due to their starch containment and lower pure latex content, however the other experimental

latex, XU 31524.00 is a bit higher. This result may due to the combination of low carboxylic acid content and low particle size. A smaller particle size and lower functionality can create a highly mobile coating.

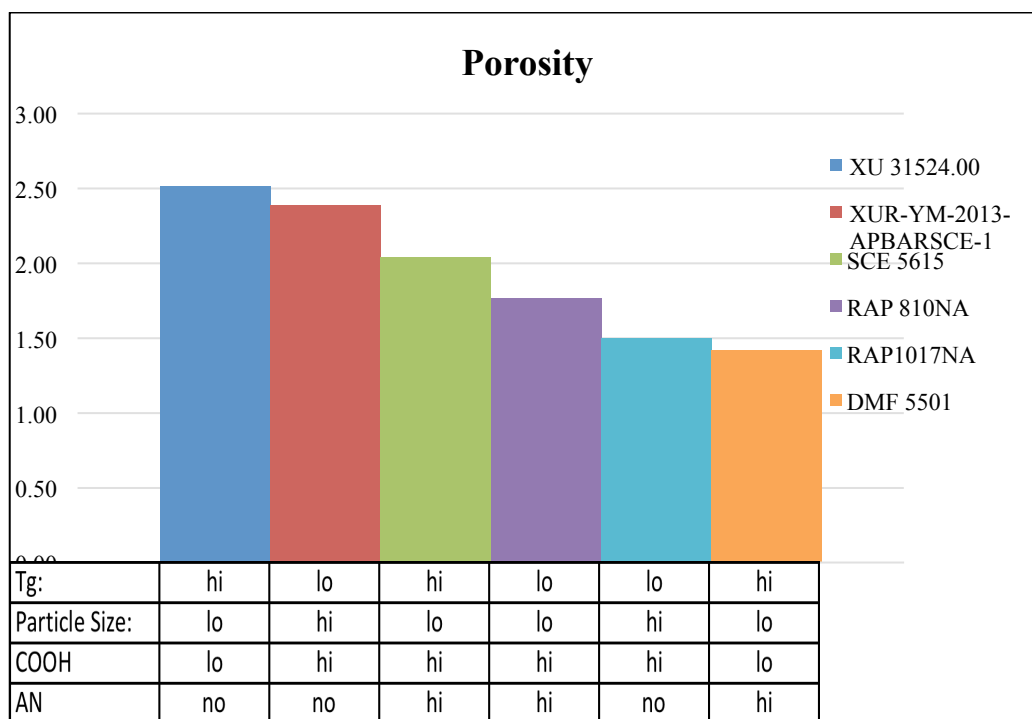


Figure 8. Porosity Summary Phase I.

The figure above shows no clear trend of porosity with Tg, particle size, carboxylic acid groups or acrylonitrile groups. However, DMF 5501 shows the lowest porosity amongst these latexes, followed by RAP 1017NA and RAP 810NA.

K&N Ink Absorption

The ink absorption test, K&N, was performed on the coated samples. Figure 9 shows a summary of these values. Measured values are very similar, indicating no significant change as a function of changes in the latex. Variation in Latexes XUR-YM-2013-APBARSCE-1, XU 31524.00 and SCE 5615 are lower in value, this can be

attributed to the starch in both XUR-YM-2013-APBARSCE-1 and SCE 5615 and the lower particle size in XU 31524.00.

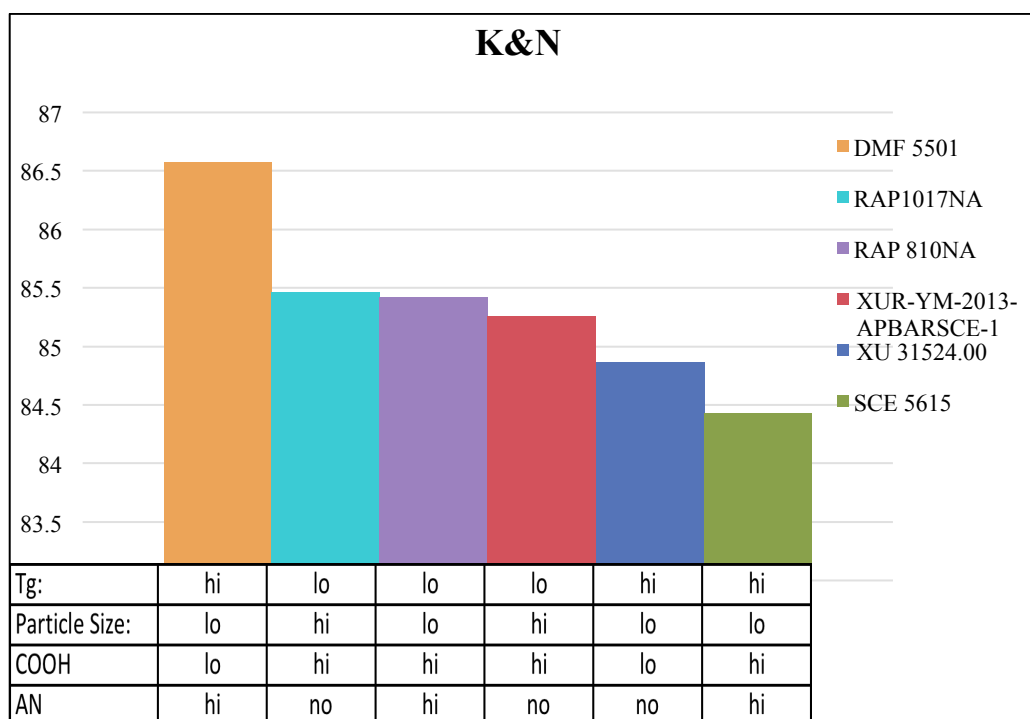


Figure 9. K&N Ink Absorption Summary Phase I.

The figure above shows the average K&N ink value as a function of the latex type, with the information about the latex properties in the table below it. The highest K&N ink value was obtained with the DMF 5501 latex, followed by RAP1017NA and RAP 810NA. The same ranking was observed with the porosity performance (lowest porosity = highest performance). As observed on examination of the latex properties, K&N ink test performance appears to correlate with low particle size and high acrylonitrile content. No clear trend is observed for Tg or carboxylic acid group content.

Croda (Manders Red Drawdown) Ink Absorption

The ink absorption test, Croda, was performed on the coated samples. Figure 10 shows a summary of these values. Measured values are within the normal expected

variation, indicating no significant change as a function of changes in the latex. Variation in Latexes XUR-YM-2013-APBARSCE-1, XU 31524.00 and SCE 5615 are lower in value, this can be attributed to the starch in both XUR-YM-2013-APBARSCE-1 and SCE 5615 and the lower particle size in XU 31524.00.

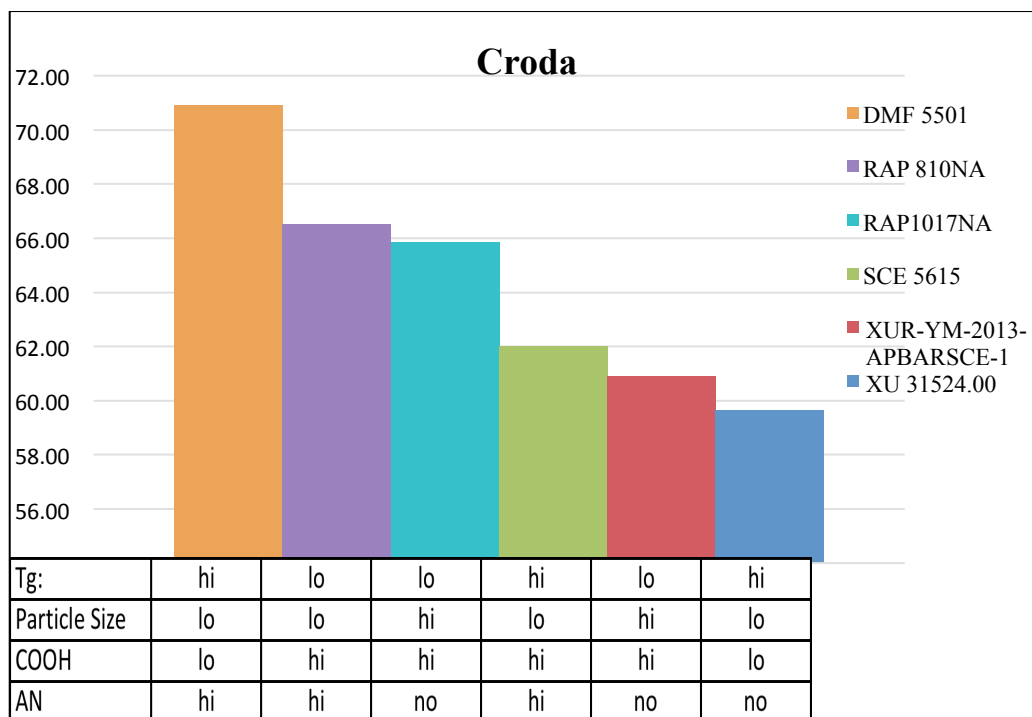


Figure 10. Croda (Manders Red Drawdown) Ink Absorption Summary Phase I.

The figure above shows the average Croda Ink value as a function of the latex type, with information about latex properties in the table below it. The highest Croda Ink value was obtained with the DMF 5501 latex, followed by RAP 810NA and RAP1017NA. The same ranking was observed with the porosity performance (lowest porosity = highest performance) and also with the Croda ink performance. As observed on examination of the latex properties, Croda ink test performance appears to correlate with low particle size and high acrylonitrile content. No clear trend is observed for Tg or carboxylic acid group content.

Surface Analysis – Scanning Electron Microscopy

The coated sheets were then analyzed using a Carl Zeiss Scanning Electron Microscope. The topography of each sheet was viewed to determine if any differences in the surfaces could be viewed.

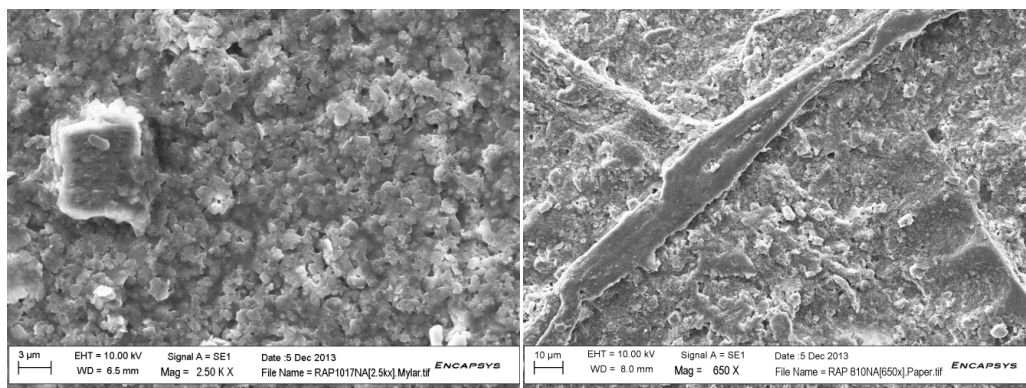


Figure 11. RAP1017NA was drawn down at 3 lbs per ream on (a) Mylar and (b) 34 lb Domtar base stock to see any significant changes in coating topography.

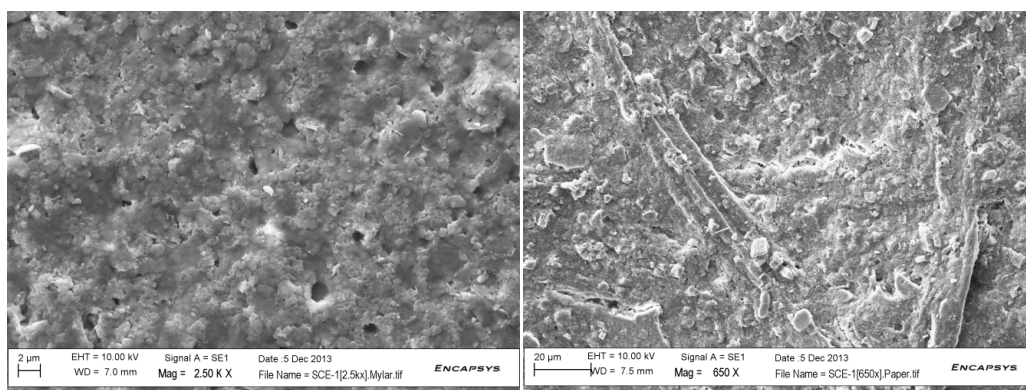


Figure 12. XUR-YM-2013-APBARSCE-1 was drawn down at 3 lbs per ream on (a) Mylar and (b) 34 lb Domtar base stock to see any significant changes in coating topography.

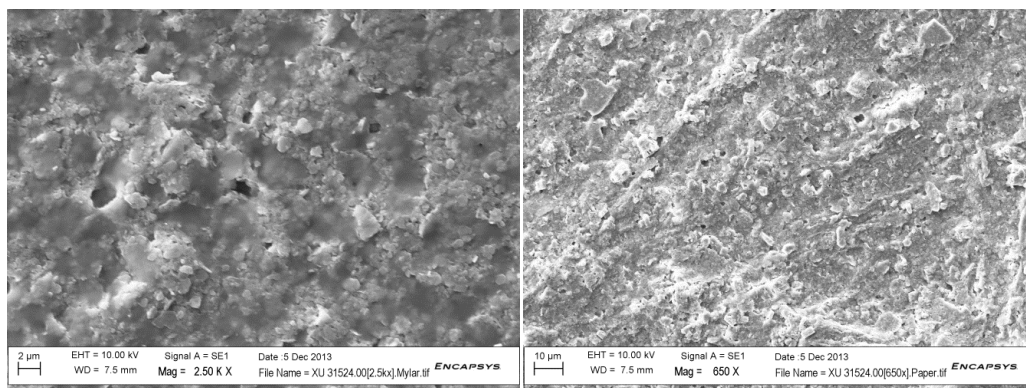


Figure 13. XU 31524.00 was drawn down at 3 lbs per ream on (a) Mylar and (b) 34 lb Domtar base stock to see any significant changes in coating topography.

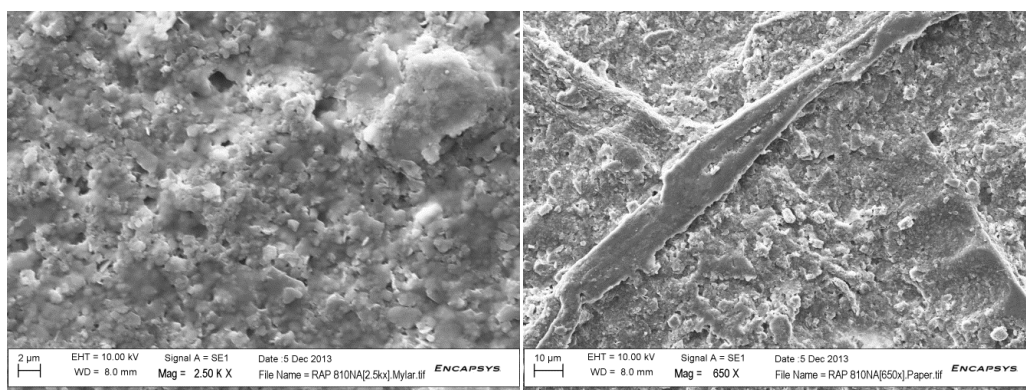


Figure 14. RAP 810NA was drawn down at 3 lbs per ream on (a) Mylar and (b) 34 lb Domtar base stock to see any significant changes in coating topography.

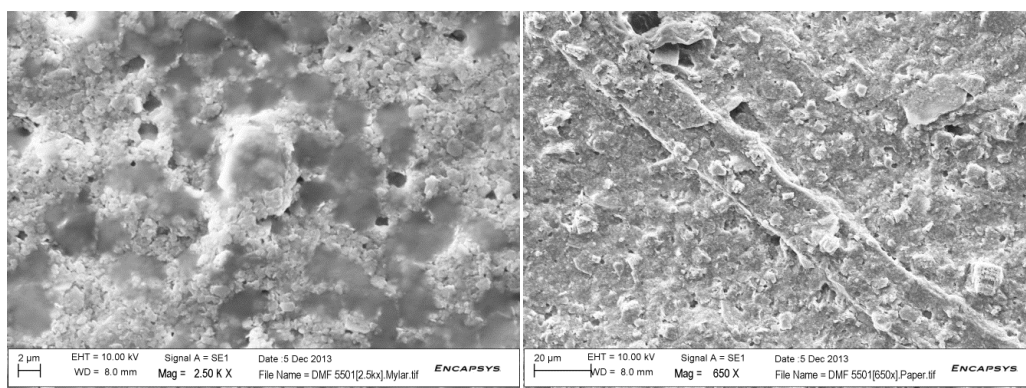


Figure 15. DMF 5501 was drawn down at 3 lbs per ream on (a) Mylar and (b) 34 lb Domtar base stock to see any significant changes in coating topography.

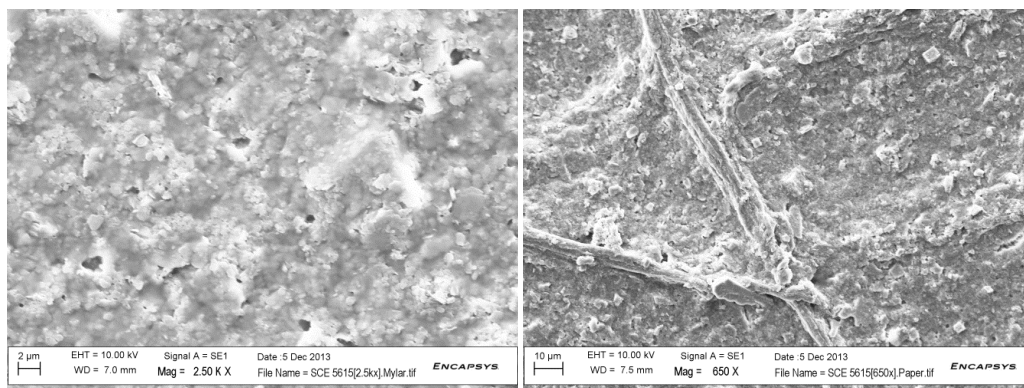


Figure 16. SCE 5615 was drawn down at 3 lbs per ream on (a) Mylar and (b) 34 lb Domtar base stock to see any significant changes in coating topography.

The coated surfaces show micron-sized rounded, raised features. The elongated features observed in the images on the right hand side (coatings on Domtar base stock) are attributed to the fibrillar nature of the paper substrate. No significant differences in the surface morphologies of the different coatings are observed. Please note that the images of the coatings on the right hand side are taken at a lower magnification of 650 x in comparison with the left taken at 2.5 kx.

With the above performance results, it was determined to move forward onto phase II continuing with the four best qualifying latexes: RAP1017NA, RAP 810NA, DMF 5501, and SCE 5615. The first three latexes are pure, and the last, SCE 5615, is a starch-containing emulsion. Latex 2, XUR-YM-2013-APBARSCE-1 containing starch, was eliminated because it showed no improvements in comparison to Latex 1, RAP1017NA containing no starch. Latex 3, XU 31524.00, was eliminated because of its high porosity.

Rheological Techniques Phase II

Fresh coatings containing RAP1017NA, RAP 810NA, DMF 5501, and SCE 5615 were created and reanalyzed.

Water Retention

The water retention value for each of the phase II coating slurries was determined using an AA-GWR Water Retention instrument and was measured when at 44% solids. Table 4 below shows the water retention summary values for the phase II tested slurries. Again no major liquid transferred values were observed, therefore no significant changes were observed for the coatings prepared from different latexes.

Table 4

Water Retention Summary Phase II

Coating Slurry	Water Retention (gm/m ²)
1. RAP1017NA	103.75
2. RAP 810NA	90.625
3. DMF 5501	105.625
4. SCE 5615	110.625

pH

pH was tested on each of the phase II coating slurry using a pH meter at 44% solids. Table 5 below shows a summary of the pH values for the phase II tested slurries. Again, it appears that the acrylonitrile groups present in the last three latex coatings below play a significant role in reducing the pH value of the coating.

Table 5

pH Summary Phase II

Coating Slurry	pH
1. RAP1017NA	7.72
2. RAP 810NA	6.66
3. DMF 5501	6.55
4. SCE 5615	6.78

Viscosity

The viscosity was measured at 44% solids for the phase II coating slurries. All values are summarized in Table 6 below. As observed in the phase I study, the starch-containing emulsion demonstrated a lower viscosity than the other formulations.

Table 6

Viscosity Summary Phase II

Coating Slurry	Viscosity (cP)
1. RAP1017NA	734
2. RAP 810NA	626
3. DMF 5501	596
4. SCE 5615	490

Performance Testing Phase II

Each of the above fresh slurry coating was drawn down on Domtar 34lb base stock of varying pounds per ream. The three varying weights were 2, 3, and 5 pounds per ream. The required performance properties were then measured.

Sheffield Porosity

Porosity of the phase II coated sheet was measured. Table 7 below is a summary of the porosity values for the phase II coated sheets. As seen below, the porosity values decrease with increasing coat weight. This was expected since a higher coat weight deposits more pore closing materials onto the porous sheet. Porosity levels between the latexes, however, are variable, with no consistent trends observed.

Table 7

Porosity Summary Phase II

2 lb Coating Slurry		Porosity (SU)
1.	RAP1017NA	0.7800
2.	RAP 810NA	0.7564
3.	DMF 5501	0.6733
4.	SCE 5615	0.5070
3 lb Coating Slurry		Porosity (SU)
1.	RAP1017NA	0.2400
2.	RAP 810NA	0.2890

Table 7 (continued).

3 lb Coating Slurry		Porosity (SU)
3.	DMF 5501	0.1088
4.	SCE 5615	0.3523

5 lb Coating Slurry		Porosity (SU)
1.	RAP1017NA	0.0716
2.	RAP 810NA	0.0561
3.	DMF 5501	0.0728
4.	SCE 5615	0.1047

K&N Ink Absorption

The ink absorption test, K&N, was performed on the phase II coated samples. Table 8 shows a summary of these values. Only very small increases in K&N values (indicating reduced ink absorbency) are observed as a function of increased coating weight. No large differences are observed between the formulations.

Table 8

K&N Ink Absorption Summary Phase II

2 lb Coating Slurry		K&N
1.	RAP1017NA	83.30

Table 8 (continued).

2 lb Coating Slurry		K&N
2.	RAP 810NA	84.48
3.	DMF 5501	84.80
4.	SCE 5615	82.53

3 lb Coating Slurry		K&N
1.	RAP1017NA	85.83
2.	RAP 810NA	86.10
3.	DMF 5501	87.66
4.	SCE 5615	83.80

5 lb Coating Slurry		K&N
1.	RAP1017NA	87.06
2.	RAP 810NA	88.43
3.	DMF 5501	88.73
4.	SCE 5615	87.66

Croda (Manders Red Drawdown) Ink Absorption

The ink absorption test Croda, was performed on the phase II coated samples. Table 9 shows a summary of these values. As observed in the K&N ink absorbency test, only small increases in Croda values (indicating decreases in ink absorption) are observed as a function of coating weight. Again, no consistent differences between the formulations are observed.

Table 9

Croda (Manders Red Drawdown) Ink Absorption Summary Phase II

2 lb Coating Slurry		Croda
1.	RAP1017NA	67.70
2.	RAP 810NA	68.20
3.	DMF 5501	71.83
4.	SCE 5615	68.76
3 lb Coating Slurry		Croda
1.	RAP1017NA	72.22
2.	RAP 810NA	71.73
3.	DMF 5501	78.66
4.	SCE 5615	70.36

Table 9 (continued).

	5 lb Coating Slurry	Croda
1.	RAP1017NA	76.63
2.	RAP 810NA	74.43
3.	DMF 5501	79.13
4.	SCE 5615	74.96

Surface Analysis – Scanning Electron Microscopy

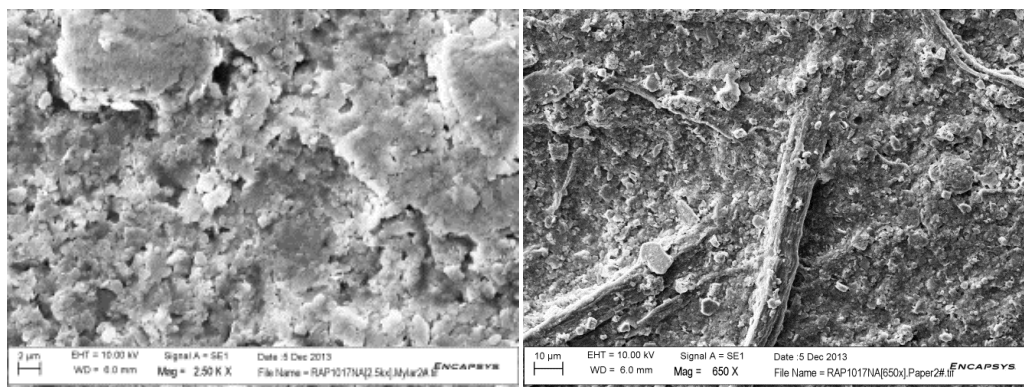


Figure 17. RAP1017NA was drawn down at 2 lbs per ream on (a) Mylar and (b) 34 lb Domtar base stock to see any significant changes in coating topography.

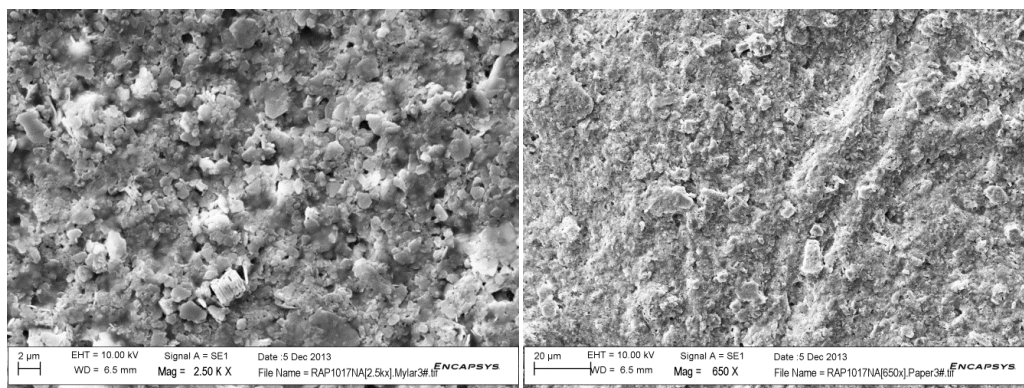


Figure 18. RAP1017NA was drawn down at 3 lbs per ream on (a) Mylar and (b) 34 lb Domtar base stock to see any significant changes in coating topography.

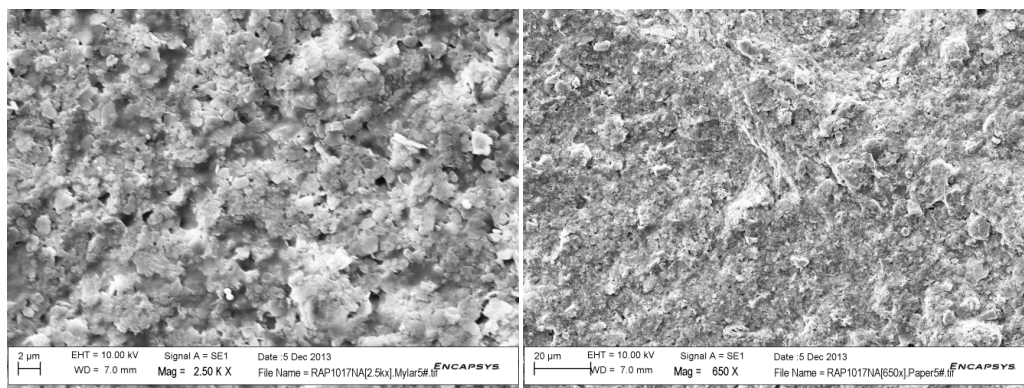


Figure 19. RAP1017NA was drawn down at 5 lbs per ream on (a) Mylar and (b) 34 lb Domtar base stock to see any significant changes in coating topography.

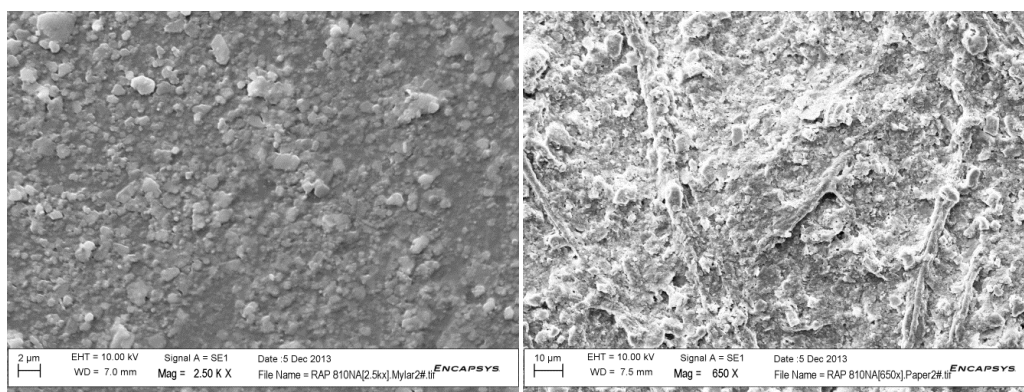


Figure 20. RAP 810NA was drawn down at 2 lbs per ream on (a) Mylar and (b) 34 lb Domtar base stock to see any significant changes in coating topography.

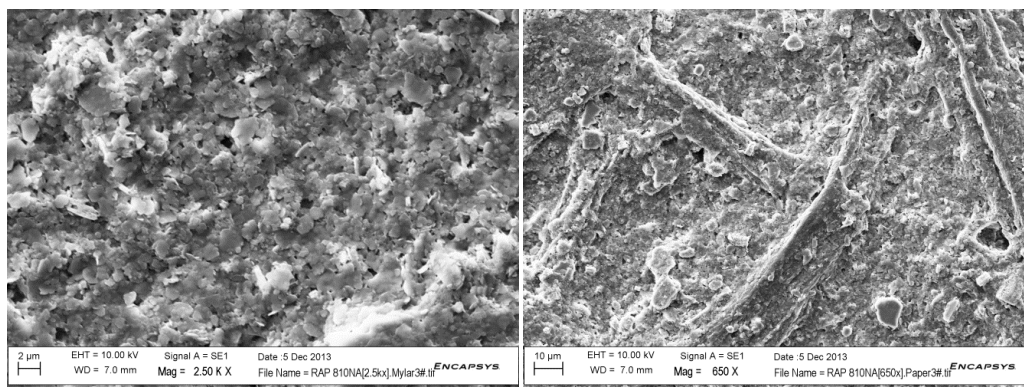


Figure 21. RAP 810NA was drawn down at 3 lbs per ream on (a) Mylar and (b) 34 lb Domtar base stock to see any significant changes in coating topography.

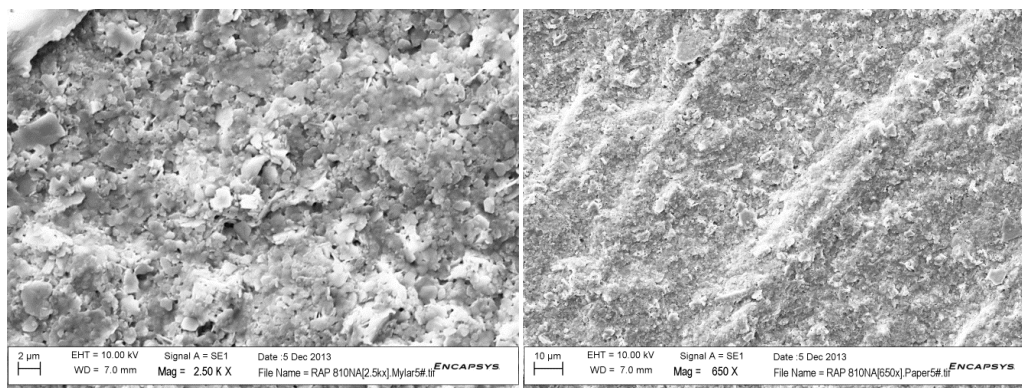


Figure 22. RAP 810NA was drawn down at 5 lbs per ream on (a) Mylar and (b) 34 lb Domtar base stock to see any significant changes in coating topography.

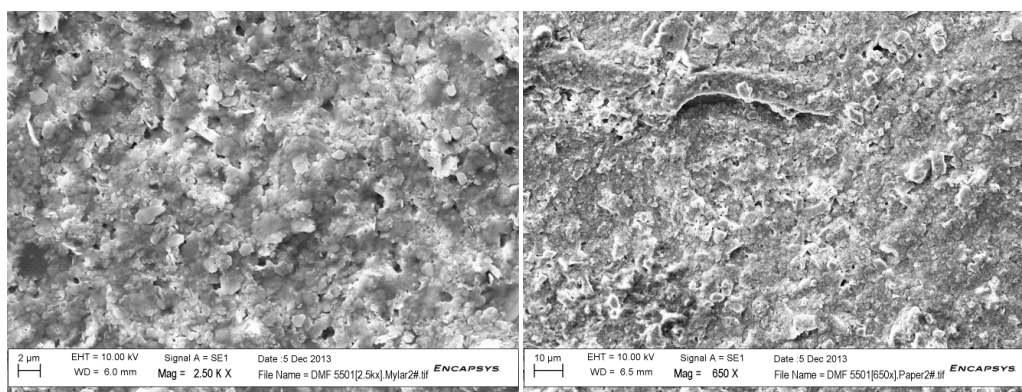


Figure 23. DMF 5501 was drawn down at 2 lbs per ream on (a) Mylar and (b) 34 lb Domtar base stock to see any significant changes in coating topography.

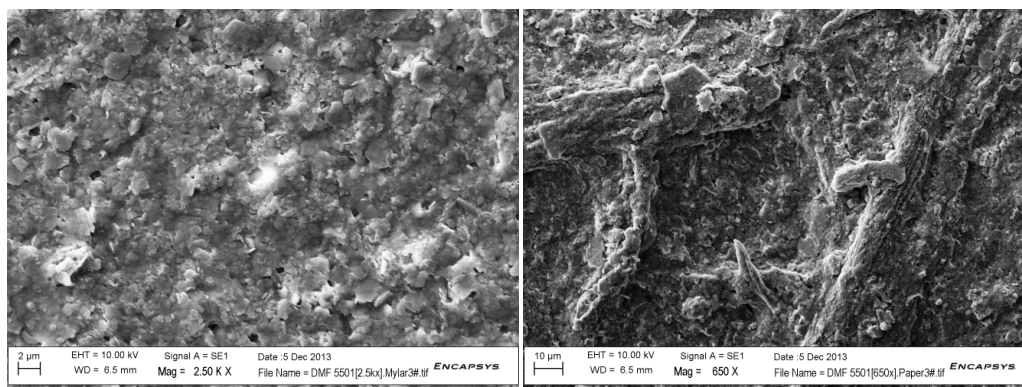


Figure 24. DMF 5501 was drawn down at 3 lbs per ream on (a) Mylar and (b) 34 lb Domtar base stock to see any significant changes in coating topography.

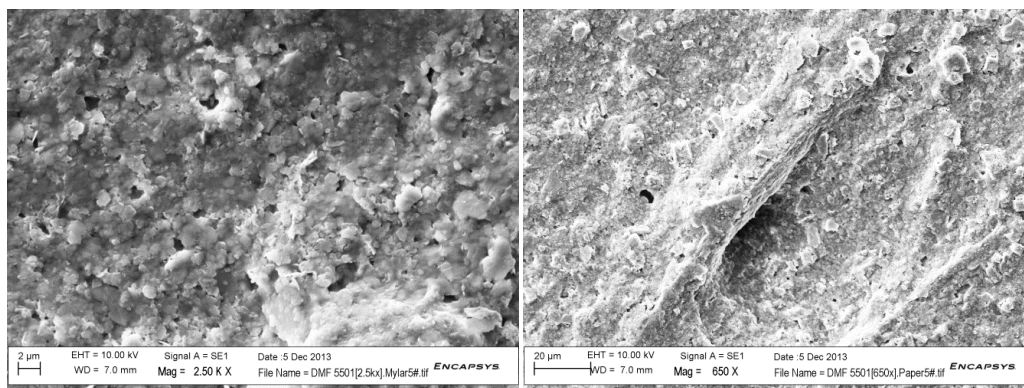


Figure 25. DMF 5501 was drawn down at 5 lbs per ream on (a) Mylar and (b) 34 lb Domtar base stock to see any significant changes in coating topography.

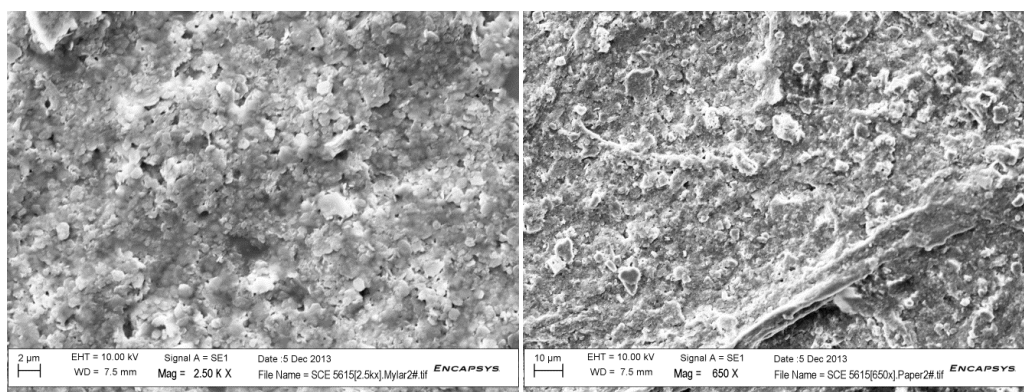


Figure 26. SCE 5615 was drawn down at 2 lbs per ream on (a) Mylar and (b) 34 lb Domtar base stock to see any significant changes in coating topography.

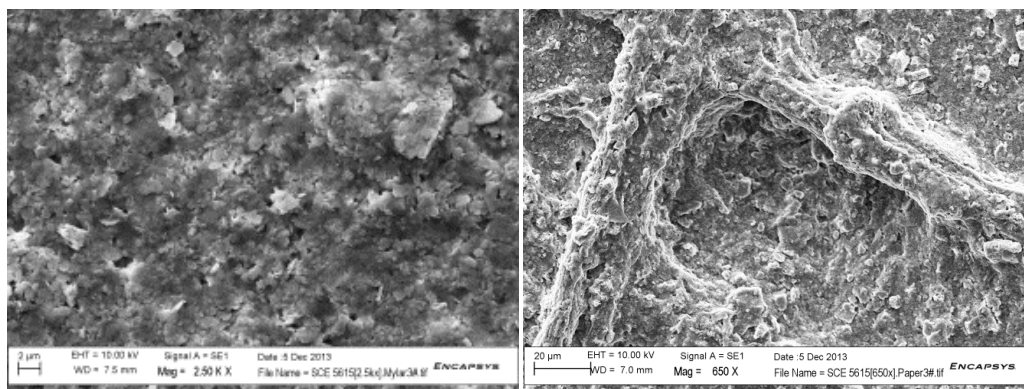


Figure 27. SCE 5615 was drawn down at 3 lbs per ream on (a) Mylar and (b) 34 lb Domtar base stock to see any significant changes in coating topography.

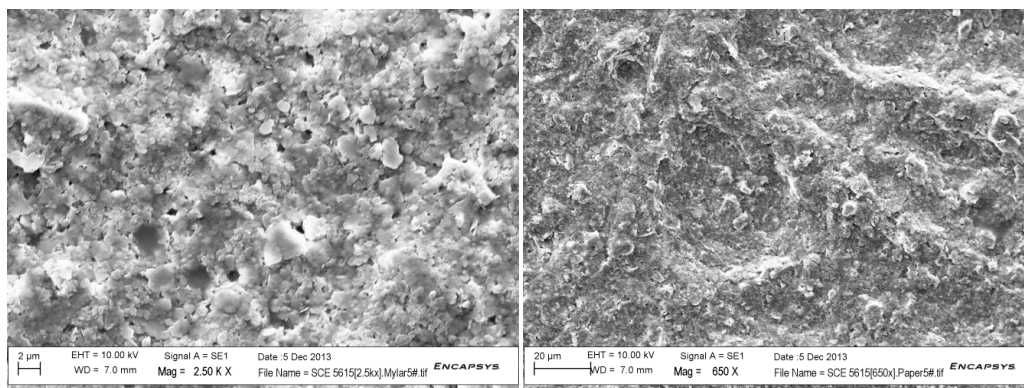


Figure 28. SCE 5615 was drawn down at 5 lbs per ream on (a) Mylar and (b) 34 lb Domtar base stock to see any significant changes in coating topography.

As observed in the Phase I SEM testing, no significant differences in surface morphology were observed as a function of latex formulation. However, for the samples coated onto Domtar base stock, as the coat weight is increased, the fibers of the base stock sheet become less visible. This is expected since a thicker coating is being applied to the base stock sheet as the coat weight increased.

Box plots of the data above were then generated using Minitab software to determine trends within the coating weight variations. The figures below show these trends.

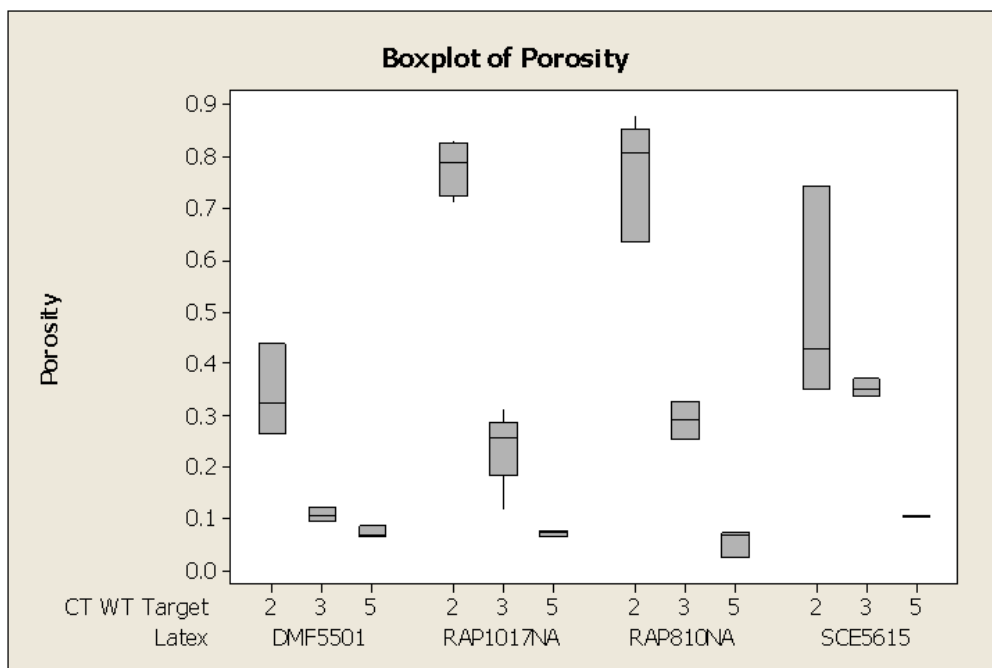


Figure 29. Box plot of Porosity.

The box plot in Figure 29 above shows that as the coat weight increases the porosity of the sheet decreases, and the variation in porosity values decreases. This trend was expected due to increasing the amount of coating being applied to the top of each sheet. With more coating applied, it is less likely any pores within the sheet will be able to remain open or free of coating. As seen above each coating demonstrates the same trend, however for the lowest coat weight of 2 lbs per ream, DMF 5501 demonstrates the lowest average porosity with the least variability.

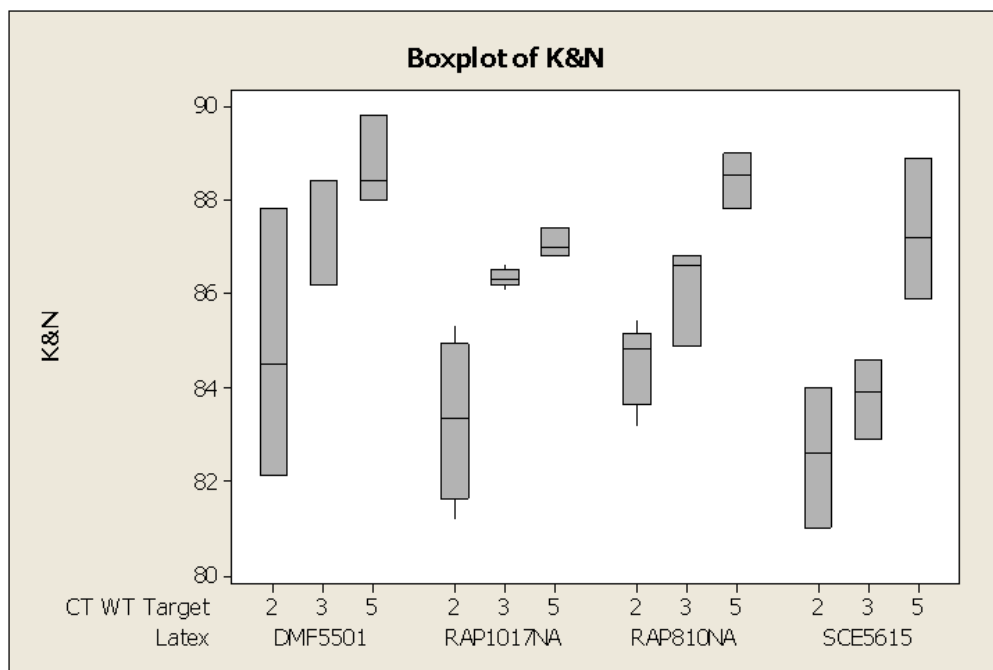


Figure 30. Box plot of K&N Ink.

The K&N Ink box plot in Figure 30 above shows a slightly different trend than porosity. With this ink absorption test, increasing the coat weight results in increases in the K&N Ink absorption values (indicating reduction in ink absorption). This result was expected, because when an increased amount of coating is applied a better film is formed, resulting in a more sealed sheet. When the sheet is sealed less of the K&N ink is absorbed into the surface of the sheet, increasing the K&N Ink value. A K&N Ink value of 100 would be a perfect white, no ink absorbed value. While similar trends are observed for each coating, the DMF 5501 and RAP810NA show higher mean values at the lowest coating weight. However, DMF 5501 shows the highest variability, so further evaluation of this coating is required.

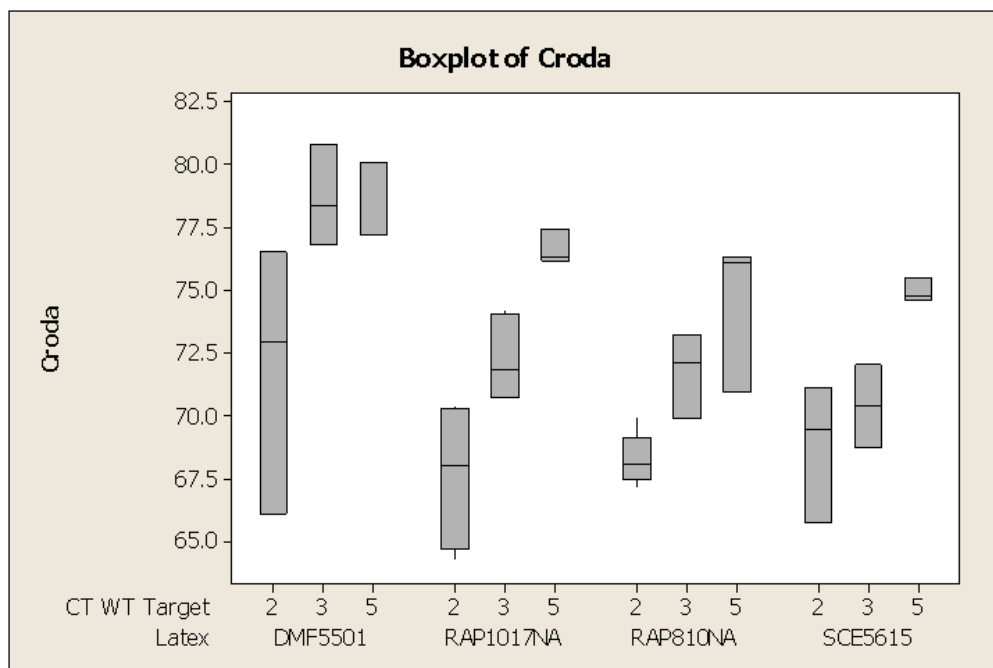


Figure 31. Box plot of Croda Ink.

The Croda Ink box plot seen in Figure 31 above shows roughly the same trend as that observed in the K&N ink absorption test. The Croda Ink test values were also expected to increase with increasing coat weight. As previously mentioned, the sheet with more coating applied forms a better film, hence a more sealed base stock sheet, thereby decreasing the absorption of the ink into the base stock sheet and increasing the Croda Ink test value to a value closer to 100. At the lowest coat weight, 2 lbs per ream, DMF 5501 provides the highest mean and the highest variability for the Croda ink value, as observed for the K&N ink test.

After the barrier coatings were analyzed both analytically and through topography, a drawdown of three pounds per ream of CB Z-30 capsule coating was applied to each of the above-mentioned samples in phase II. The performance verification tests were then performed to determine their suitability for use as carbonless paper.

Performance Verification Analysis

2 Minute Typewriter Intensity

Two minute Typewriter Intensity image testing was done for each barrier coated/CB capsule-coated samples. Table 10 below shows the summary of these values. The values below are within range of the normal values obtained for good quality image intensity. The desired outcome for TI is in the range of 40-50. Measured values within this range indicate that the intensities are neither too hot nor too cold. Figure 32 below shows a photograph of the actual images obtained with each sample tested in the 2 minute typewriter intensity test. Very little difference between the samples can be seen.

Table 10

2 Minute Typewriter Intensity Imaging Summary

RAP1017NA Barrier Coat Weights		2 Minute Typewriter Intensity
1.	1.7	40.8
2.	2.85	44.95
3.	4.95	47.45
RAP 810NA Barrier Coat Weights		2 Minute Typewriter Intensity
1.	1.6	47.95
2.	2.4	45.8
3.	5.3	49.4

Table 10 (continued).

DMF 5501 Barrier Coat Weights		2 Minute Typewriter Intensity
1.	2.05	47.45
2.	2.9	41.95
3.	5.1	49.25

SCE 5615 Barrier Coat Weights		2 Minute Typewriter Intensity
1.	1.85	46.7
2.	2.8	47.95
3.	5.3	47.95



Figure 32. Typewriter Intensity Sample Images – Images going from top to bottom, RAP1017NA, RAP 810NA, DMF 5501 and SCE 5615.

Based on the above results, if targeting the lowest coat weight, at 2 lbs per ream, RAP1017NA seems to produce the lowest value for intensity, hence creating a darker image. RAP 810NA, DMF 5501 and SCE 5615 are not far from this value, however a darker image is visible when comparing RAP1017NA to the other images of the samples.

Frictional Smudge

Frictional smudge image testing was done on each barrier coated/CB capsule-coated samples. Table 11 below shows the frictional smudge imaging summary of the values obtained. The values shown are within normal range; the closer the value is to

100, the stronger the capsules are at withstanding more frictional pressure. The lower the value, the darker the image will be, and therefore, breakage of the capsules is achieved more easily. Figure 33 below provides a photograph of the images of each sample tested in the frictional smudge test. Very little difference is observed by the eye, however the opacimeter provides differentiation.

Table 11

Frictional Smudge Imaging Summary

RAP1017NA Barrier Coat Weights		Frictional Smudge
1.	1.7	83.55
2.	2.85	81.5
3.	4.95	75.95

RAP 810NA Barrier Coat Weights		Frictional Smudge
1.	1.6	80.45
2.	2.4	79.2
3.	5.3	88

DMF 5501 Barrier Coat Weights		Frictional Smudge
1.	2.05	75.75

Table 11 (continued).

DMF 5501 Barrier Coat Weights		Frictional Smudge
2.	2.9	82.5
3.	5.1	76.25

SCE 5615 Barrier Coat Weights		Frictional Smudge
1.	1.85	78.25
2.	2.8	76.55
3.	5.3	77.7

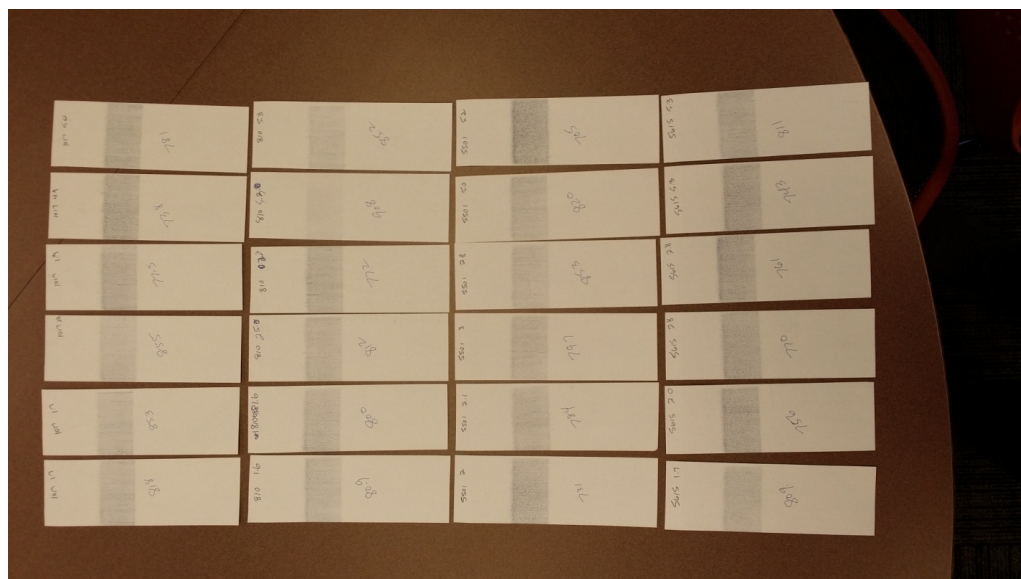


Figure 33. Frictional Smudge Sample Images - Images going from left to right, RAP1017NA, RAP 810NA, DMF 5501 and SCE 5615.

Based on the above results, it can be concluded that as the amount of coating applied to the base stock sheet increases, the probability of the capsules breaking increases, resulting in a darker image and a lower intensity value for the RAP1017NA and SCE 5615 latexes. For the RAP1017NA coating this may be attributed to the higher particle size of the latex. For the SCE 5615, this may be attributed to the presence of the starch within the latex. A very different trend is seen in the RAP 810NA and DMF 5501 coatings. In this case, increase in coating weight results in an increase in the intensity value, indicating less breakage of capsules. These trends may be attributed to the lower particle size, better flowing, more mobile film, and the presence of greater concentrations of acrylonitrile groups creating better binding properties between the barrier coating and the CB capsule coating.

CHAPTER IV

CONCLUSIONS

In order to better understand the structure-property relationships of the components within a slurry coating affecting the performance properties of a barrier coated sheet, this thesis investigated latexes of different compositions, different particle sizes, and different glass transition temperatures. In doing this, six different latexes were analyzed; four latex and two starch containing emulsion latexes containing varying amounts of carboxylic acid groups and acrylonitrile groups, with different particle sizes and Tgs.

Several different tests were done on both the slurry coating, barrier coated sheets, and barrier coated + CB capsule coated samples. These tests included:

- Slurry Coating: Water retention, Viscosity and pH
- Barrier Coated Sheets: Porosity, K&N Ink Test, and Croda Ink Test
- Barrier Coated + CB Capsule Coated sheets: 2 Minute Typewriter Intensity and Frictional Smudge

These tests help to verify the original hypothesis of the formulation parameters that would determine the effectiveness of the barrier coating. These parameters include:

- Nitriles improve binding, and produce a softer, more pliable coating with higher strength
- Carboxylic acid groups improve the binding properties
- Smaller particle size is usually preferred to provide better flow and coating, however this can also create more mobile particles

This research has generated some general conclusions. First, increasing barrier coating (sub-coat) weight, improves the sub-coat barrier properties. Second, smaller particle size latexes create a better film and more sealed base stock sheet; this was observed not only in the porosity values, but also in the ink absorption results. Third, it was determined that acrylonitrile-containing latexes perform better when they presence in the latex, due to the hydrogen bonding that develops, increasing the bond strength interaction with the sheet fibers and other coating ingredients to produce hydrogen bonds and improve the binding ability of the latex to the base stock sheet. Lastly, the carboxylic acid groups in the chosen latexes have helped to increase bond strength with the fibers, hence increasing the coatings' ability to adhere to the fiber surface of the base stock sheet.

The results of this research demonstrated that, DMF 5501 was the best performing latex of those evaluated when targeting lower coat weights of 2 or 3 lbs per ream. The smaller particle size and presence of carboxylic acid and acrylonitrile groups in this formulation seem to aid in the improved performance at lower coat weight. An increase in binder efficiency, attributed the presence of both the carboxylic acid and acrylonitrile groups, was seen. These groups increase the binding of the CB capsule coating to the base stock sheet. The smaller particle size aids in this binding by creating a better flowing, more pliable latex which creates an evenly formed barrier coat film. The porosity values show that DMF 5501 forms a better film, creating a more sealed sheet, and thus demonstrates the lowest porosity value on the coated sheet. The K&N and Croda Ink intensity values also show that DMF 5501 performs best by creating the highest ink intensity values on each base stock sheet. The performance verification tests indicated that if DMF 5501 latex was used within the current carbonless paper product at only 2 lbs

per ream of applied coating, the product performs within the required standards set by Appleton Paper Inc.

Future Research Considerations

The results of this research gave a basic understanding of the structure-property relationships controlling the performance of a barrier coated base stock sheet and a CB capsule coating. However, more research must be done before making changes to commercial products. The following experiments may be considered for a future research study.

Evaluate the effectiveness of the DMF 5501 latex with less binder within the coating. Since it was shown through this research that the DMF 5501 is sealing the sheet better producing better binder efficiency, less binder may be needed in the actual coating to help regain some of the lost intensity values. Doing this can produce a better sealed sheet with higher intensity values and could also lower the costs associated with creating the coating.

A study to understand the effects of changing ratios of pigment, latex and starch in an SCE latex is needed. The current study indicated that these ratios are not optimized, as the SCE latexes underperformed in comparison to the DMF 5501. These studies will determine if properties can be improved while reducing the costs of the coating.

APPENDIX

LATEX AND BARRIER COAT DATA

Latex Data	RAP1017NA	XUR-YM-2013-APBARSCE-1	XU 31524.00	RAP 810NA	DMF 5501	SCE 5615
Chemistry	Styrene Butadiene	Styrene Butadiene	Styrene Butadiene	Styrene Acrylic	Styrene Butadiene	Styrene Butadiene
Carboxylic acid	Moderate	Moderate	Low	Moderate	Low	Moderate
Acrylonitrile	none	none	none	High	High	High
SCE	no	yes	no	no	no	yes
Particle size	230 nm	230 nm	125 nm	155 nm	135 nm	135 nm
pH	8	7.5	8	6.5	6.5	6.5
Percent Solids	48.80%	48.30%	52.00%	48.00%	49.00%	50.00%
Tg (deg C)	-6	-4	17	-2	15	14
MFFT (deg C)	9	10	17	2	18	18
Gel %	87	86	86	91	83	80

Phase I Coatings	RAP1017NA	XUR-YM-2013-APBARSCE-1	XU 31524.00	RAP 810NA	DMF 5501	SCE 5615
Adjusted Solids	44.75%	44.81%	44.67%	44.84%	44.62%	44.33%
Water Retention (gm/m²)	105.42	100.42	102.5	90	104.58	115.83
pH	7.74	7.73	7.84	6.88	6.81	6.96
Viscosity (cP)	450	402	436	440	390	244

Phase II Coatings	RAP1017NA	RAP 810NA	DMF 5501	SCE 5615
Adjusted Solids	44.14%	44.31%	43.99%	44.02%
Water Retention (gm/m²)	103.75	90.63	105.63	110.63
pH	7.72	6.66	6.55	6.78
Viscosity (cP)	734	626	596	490

REFERENCES

- (1989). *Technical manual carbonless rolls*. Appleton, WI: Appleton Papers Inc.
- Appleton Papers Inc. (2012). *Coating conference*. Paper presented at Appvion Inc. Coating Conference, Appleton, WI.
- Appleton Papers Inc. (2013). *Appvion Library Tech Support Questions* From <http://www.appvion.com>
- Appvion (Ed.). (2013). *Carbonless sheets technical solutions handbook*. Retrieved 2013, From Appvion.com website: http://appvion.com/enus/products/carbonless/Documents/Carbonless%20Sheets/Sheet_Tech_Solutions_Handbook.pdf
- Ball, D. W. (2012). *Physical Chemistry*. Pacific Grove, CA: Brooks/Cole-Thompson Learning Inc.
- Blackley, P. C. (1975). *Emulsion polymerization theory and practice*. Barkley, London: Applied Science Publishers.
- Bollstrom, R., Tuominen, M., Maattanen, A., Peltonen, J., & Toivakka, M. (2011). Top layer coat ability on barrier coatings. *Tappi Journal PaperCon*. p 511-521.
- Bollstrom, R., Nyqvist, R., Preston, J., Salminen, P., & Toivakka, M. (2013). Barrier Properties created by Dispersion Coating. *Tappi Journal*. 12(4), p 45-51.
- Burrell, M. M. (2003). Starch the need for improved quality or quantity - an overview. *Journal of Experimental Biology*, 54(382), p 451-456.
- Dillard, D.A. & Pocius, A. (2002). *The Mechanics of Adhesion. Adhesion Science and Engineering – I*. Netherlands: Elsevier Science B.V.

- Everett, D.H. (1992). IUPAC – division of physical chemistry, manual of symbols and terminology for physicochemical quantities and units – appendix II: definitions, terminology and symbols in colloid and surface chemistry. *Pure and Applied Chemistry*. 31(9), p 44.
- Fouassier, J.P. (1993). *Radiation Curing In Polymer Science and Technology*. England: Kluwer Academic Publishers.
- Freitag, W. & Stoye, D. (1996) *Resins for Coatings: Chemistry, Properties and Applications*. Cincinnati: Hanser/Gardner Publications, Inc.
- Glatfelter 2005. *Technical Bulletin*. Issue 2005-3.
- Glatthaar, R. (2011). *Technical handbook carbonless papers*. Bielefeld, Germany: Mitsubishi HiTec Paper Europe GmbH.
- Golden, R. et al. (1979), *U.S. Patent No. 4,154,462*. Washington, DC: U.S. Patent and Trademark Office.
- Golden, R. (1983), *U.S. Patent No. 4,381,120*. Washington, DC: U.S. Patent and Trademark Office.
- Hertz Jr., D.L., & Bussem, H. (1994). *Nitrile Rubber – Past, Present & Future*. Rubber Division, American Chemical Society. Pittsburgh, Pennsylvania. Paper No. 58.
- Hubbe, M. Mini-Encyclopedia of Papermaking Wet-End Chemistry. *NC State University* Retrieved from <http://www4.ncsu.edu/~hubbe/STCH.htm>.
- Karukstis, K. K., & Vanlecke, G. R. (2003). *Chemistry connections the chemical basis of everyday phenomena* (2nd ed.). San Diego, CA: Academic Press.

- Kjellgren, H. (2008). *Barrier properties of greaseproof paper* (Unpublished master's thesis). Karlstad University, Sweden.
- Laurence, K. M. (1995). The exciting history of carbonless paper. Retrieved March 24, 2013, from The Exciting History of Carbonless Paper website:
<http://www.kevinlaurence.net/essays/cc.php>
- Mackawic, V., Alol, F. & Trksak, R. (2000) *A Different Way to Look at Surface Starch for Improved Film Formation and Barrier Properties*. Papermakers Conference Proceedings.
- Marinelli, N. (1985). *U.S. Patent No. 4,533,567*. Washington, DC: U.S. Patent and Trademark Office.
- Morabito, P. (2008), *U.S. Patent No. 7,320,825*, Washington, DC: U.S. Patent and Trademark Office.
- Mumford, J. (2007, December 3). *How carbonless paper works*. Retrieved 2013, from Ezine Articles website: <http://ezinearticles.com/?How-Carbonless-Paper-Works&id=996064>
- Salamone, J. C. (n.d.). Thermosensitive paper (thermosensitive dyes, thermochromic compounds). *T-Z: Polymeric materials encyclopedia* (Vol. 11, pp. 8369-8374). Danvers, MA: CRC Press Inc.
- Scott, W. E., & Trosset, S. (1989). *Properties of Paper: An Introduction*. Atlanta, GA: Tappi Press.
- Seitz, M. (1992), *U.S. Patent No. 5,132,271*, Washington, DC: U.S. Patent and Trademark Office.

Shin, J., Jones, N., Lee, D., Fleming, P., Joyce, M.

DeJong, R. & Bloembergen, S. (2012). Rheological Properties of Starch Latex Dispersions and Starch Latex-Containing Colors. *Tappi Journal PaperCon*. p 986-1009.

Tappi routine control methods. (n.d.). In *Technical association of pulp and paper industries*. Retrieved 2013, From http://kandnlaboratories.com/KandN_Testing_Ink_files/TAPPI.pdf

Torraspapel, S.A. (2008) *About Paper Carbonless Paper*. Barcelona, Spain: Torraspapel.

Tracton, A. A. (2007) *Coating Materials and Surface Coatings*. Boca Raton: FL: CRC Press: Taylor & Francis Group, LLC.

Troedel, M. L. *Methods For Testing High Barrier Materials*. MAS Consulting Services. From http://www.tappi.org/content/pdf/member_groups/Packaging/PLC99305.pdf

Vaha-Nissi, M., Savolaninen, A., Talja, M. & Moro, R. (1998). Dispersion barrier coating of high-density base papers. *Tappi Journal*. 81(11).

White, M. A. (1998). The Chemistry behind Carbonless Copy Paper. *Journal of Chemical Education*. 75(9), p 1119-1120.

Wu, N., J. Parris. (2000). Interaction of water-soluble acrylic polymers with alcohols in aqueous solutions. *Colloids and Surfaces A: Physicochemical and Engineering Aspects*. 167(1), p 179-187.

Wygant, R. W. (2011). *Measurement and effects of paper coating structure*. In ECC international technology center. Retrieved 2013, From <http://roger.wygant.org/subdomains/roger/publications/Measurement%20and%20Effects%20of%20Coating%20Structure.pdf>

Zang, Y. H., & Aspler, J. S. (1995). The influence of coating structure on the ink receptivity and print gloss of model clay coatings. *Tappi journal* (78th ed.). Retrieved 2013, From <http://www.tappi.org/Downloads/unsorted/UNTITLED-95Jan147pdf.aspx>